Virus Research 160 (2011) 108–119

Contents lists available at ScienceDirect

Virus Research

journal homepage: www.elsevier.com/locate/virusres

Puumala virus infection in Syrian hamsters (*Mesocricetus auratus*) resembling hantavirus infection in natural rodent hosts

Takahiro Sanada[a], Hiroaki Kariwa[a,*], Noriyo Nagata[b], Yoichi Tanikawa[a], Takahiro Seto[a], Kumiko Yoshimatsu[c], Jiro Arikawa[c], Kentaro Yoshii[a], Ikuo Takashima[a]

[a] Graduate School of Veterinary Medicine, Hokkaido University, Sapporo, Hokkaido 060-0818, Japan
[b] Department of Pathology, National Institute of Infectious Diseases, Tokyo 208-0011, Japan
[c] Graduate School of Medicine, Hokkaido University, Sapporo, Hokkaido 060-0838, Japan

ARTICLE INFO

Article history:
Received 23 April 2011
Received in revised form 28 May 2011
Accepted 28 May 2011
Available online 6 June 2011

Keywords:
Hantavirus
Puumala virus
Animal model
Persistent infection
Hamster

ABSTRACT

The mechanism of hantavirus persistent infection in natural hosts is poorly understood due to a lack of laboratory animal models. Herein, we report that Syrian hamsters (*Mesocricetus auratus*) infected with Puumala virus (PUUV) at 4 weeks old show persistent infection without clinical symptoms for more than 2 months. IgG and IgM antibodies against the viral nucleocapsid protein and neutralizing antibody were first detectable at 14 days postinoculation (dpi) and maintained through 70 dpi. Viral RNA was first detected from 3 dpi in lungs and blood clots, and was detected in all tissues tested at 7 dpi. The viral RNA persisted for at least 70 days in the lungs, kidney, spleen, heart, and brain. The highest level of RNA copies was observed at 14 dpi in the lungs. Slight inflammatory reactions were observed in the lungs, adrenal glands, and brain. Immunohistochemical analysis revealed that PUUV antigen persisted until 56 dpi in the kidneys and adrenal glands. Infected hamsters showed no body weight loss or clinical signs. These results indicate that PUUV infection in hamsters is quite similar to the hantavirus infection of natural host rodents.

1. Introduction

Hantaviruses, which belong to the family *Bunyaviridae*, are distributed worldwide and carried by a variety of rodent and insectivore species (Jonsson et al., 2010). Hantaviruses possess a trisegmented, negative-stranded RNA genome consisting of small (S), medium (M), and large (L) segments (Plyusnin et al., 1996), which encode nucleocapsid proteins (N), envelope glycoproteins (Gn and Gc), and RNA-dependent RNA polymerase, respectively (Plyusnin et al., 1996). Hantaviruses cause two human diseases: hemorrhagic fever with renal syndrome (HFRS) and hantavirus cardiopulmonary syndrome (HCPS) (Jonsson et al., 2010). The clinical symptoms of HFRS are characterized by fever, renal failure, and hemorrhage with capillary leakage (Muranyi et al., 2005). HFRS occurs mainly in Asia and Europe, with 150,000–200,000 cases annually (Jonsson et al., 2010; Muranyi et al., 2005), and its case fatality rate is 0.1–15% (Kanerva et al., 1998; Muranyi et al., 2005). Hantaan virus (HTNV), Seoul virus (SEOV), Amur virus (AMRV), Dobrava-Belgrade virus (DOBV), Saaremaa virus (SAAV), and Puumala virus (PUUV) have been identified as etiologic agents of HFRS, and they are each carried by a specific rodent species: striped field mouse, *Apodemus agrarius*; Norway rat, *Rattus norvegicus*; Korean field mouse, *Apodemus peninsulae*; yellow necked mouse, *Apodemus flavicollis*; striped field mouse, *Apodemus agrarius*; and bank vole, *Myodes glareolus*, respectively (Jonsson et al., 2010). HCPS is characterized by fever and severe cardiopulmonary dysfunction (Muranyi et al., 2005). Sin Nombre virus (SNV), Laguna Negra virus (LNV), and Andes virus (ANDV) are considered to be the major pathogens of HCPS (Bi et al., 2008; Jonsson et al., 2010). The case fatality rate of HCPS is as much as 50% (Muranyi et al., 2005).

In contrast to human infections, hantaviruses are generally believed to infect natural hosts persistently and are nonpathogenic to their reservoir hosts (Gavrilovskaya et al., 1990; Yanagihara et al., 1985). Although an immune response to the virus is induced, the natural hosts harbor viral RNA and antigens, especially in the lungs, and maintain the virus for over a year after infection (Gavrilovskaya et al., 1990; Lee et al., 1981; Yanagihara et al., 1985). The virus is shed in rodent excreta, such as urine, feces, and saliva, which are believed to represent the major source of hantavirus infection in humans by inhalation (Lee et al., 1981; Vapalahti et al., 2003; Yanagihara et al., 1985).

* Corresponding author at: Graduate School of Veterinary Medicine, Hokkaido University, Kita-18 Nishi-9, Kita-ku, Sapporo, Hokkaido 060-0818, Japan.
Tel.: +81 11 706 5212; fax: +81 11 706 5212.
E-mail address: kariwa@vetmed.hokudai.ac.jp (H. Kariwa).

0168-1702/$ – see front matter © 2011 Elsevier B.V. All rights reserved.
doi:10.1016/j.virusres.2011.05.021

The mechanisms for persistent infection of hantaviruses in their natural hosts remain unclear. One factor that impedes the clarification of these mechanisms is a lack of animal models. To date, no laboratory animal model is persistently infected with hantavirus that shows no clinical signs as natural hosts. Some researchers have used colonized wild rodents for analyzing the kinetics of hantavirus in natural hosts (Botten et al., 2000; Gavrilovskaya et al., 1990; Hardestam et al., 2008; Lee et al., 1981; Yanagihara et al., 1985), but four major problems exist associated with the use of wild rodents species in laboratory experiments. First, wild rodents should be handled and bred with specialized technical skill. Second, wild rodents have a diverse genetic background. Third, microbiological control is difficult in wild rodents because they are potential carriers of various microbes. And fourth, few research tools are available to analyze wild rodents. Therefore, developing animal models of hantavirus persistent infection is necessary using common laboratory animals.

In this study, we report that Syrian hamsters infected at 4 weeks old with PUUV, which is the etiologic agent of HFRS, showed persistent infection. Despite a high level of antibodies against PUUV, the animals harbored high levels of viral RNA in the acute phase of infection and maintained the virus in lungs for 70 days postinoculation (dpi). Viral RNA and antigens were also detected in some organs, but the hamsters showed no signs of illness. These data suggest that the Syrian hamster could be a suitable animal model resembling hantavirus persistent infection in the natural host.

2. Materials and methods

2.1. Cells and virus

The Sotkamo strain of PUUV was propagated in Vero E6 cells. Cells were cultivated in Eagle's minimum essential medium (EMEM) supplemented with 10% fetal bovine serum, 2 mM L-glutamine, 100 IU/ml penicillin, and 100 μg/ml streptomycin at 37 °C in a 5% CO_2 incubator. Following incubation for 14 days, the culture fluid from the cell monolayer was collected as the virus stock and stored at −80 °C until use.

2.2. Animals

Four-week-old (subadult) and 8-week-old (adult) male Syrian hamsters (SLC Inc., Hamamatsu, Japan) were inoculated subcutaneously with 3,300 focus-forming units (FFU) or EMEM as control. Hamsters were observed daily and their body weight was measured. 2–3 animals from 4-week-old group were killed on 3, 7, 14, 28, 42, 55, or 70 dpi, and 3 to 5 animals from 8-week old group were killed on 3, 7, 14, 28, 42, 56, or 70 dpi. Their internal organs (brain, heart, lung, liver, spleen, and kidney) and sera were collected and stored at −80 °C until analysis. All animal experiments were performed according to the guidelines of animal experimentation at the School of Veterinary Medicine, Hokkaido University, and carried out at a biosafety level 3 animal facility.

2.3. Antibody

The mouse monoclonal antibody E5/G6 against HTNV N and cross-reactive with PUUV N was obtained by immunization with HTNV-infected cell lysate (Yoshimatsu et al., 1996).

2.4. Indirect immunofluorescent antibody test (IFA)

The sera were tested for antibodies to PUUV using an IFA method. Vero E6 cells were infected with Puumala virus Sotkamo strain and cultured for 21 days. The infected cells were collected by trypsinization and spotted onto 24-well slides. After incubation for 4 h in a CO_2 incubator, the cells were fixed with cold acetone for 20 min and air-dried. The slides were stored at −40 °C until use. Hamster sera were diluted serially by twofold (starting at 1:16) with phosphate-buffered saline (PBS) and spotted onto the slide. After incubation at 37 °C for 1 h, the slides were washed three times with PBS. Alexa Fluor® 488 conjugated anti-hamster IgG (Invitrogen, Carlsbad, CA, USA) diluted 1:1000 in PBS was spotted on the slides and incubated at 37 °C for 1 h. The IFA titers of each serum were determined as the reciprocal of the maximum dilution of serum that yielded scattered granular fluorescence in the cytoplasm.

2.5. IgG detection enzyme-linked immunosorbent assay (IgG-ELISA)

Recombinant N (rN) of Hokkaido virus (Kariwa et al., 1995) was expressed as a fusion protein with N-utilization substance A (NusA) by cloning into the pET-43.1c(+) vector (Novagen, San Diego, CA, USA) and purified using the ProBond™ purification system (Invitrogen). Then 96-well EIA/RIA plates (Corning Inc., Corning, NY, USA) were coated overnight at 4 °C with 50 μl per well of the rN or the NusA diluted in PBS at a concentration of 1.6 μg/ml. The coated plates were blocked with 200 μl per well of 3% bovine serum albumin (BSA) in PBS at 37 °C for 1 h, followed by washing three times with PBS containing 0.5% Tween 20 (PBST); then 50 μl of the serum samples diluted to 1:200 in PBST were added to the plates. Each serum sample was reacted with the rN and the NusA protein. After 1 h of incubation at 37 °C, the plates were washed three times with PBST. The plates were then incubated with 50 μl of peroxidase conjugated anti-hamster IgG diluted to 1:1,000 in PBST at 37 °C for 1 h. After washing, 100 μl of *o*-phenylenediamine substrate with hydrogen peroxide was added to each well, and the plates were incubated at 37 °C for 30 min. The absorbance was then measured at 450 nm and the value for each sample in the well with NusA was subtracted from that of the corresponding well containing rN.

2.6. Preparation of antigens for IgM detection ELISA (IgM-ELISA) and N detection ELISA (N-ELISA)

Monolayers of Vero E6 cells were infected with the Sotkamo strain of PUUV and incubated for 14 days. After centrifugation at 100 × *g* for 2 min, the cells were resuspended in lysis buffer (0.01 M Tris–HCl, 2% Triton X-100, 0.15 M NaCl, 0.6 M KCl, 5 mM EDTA) to 2×10^7 cells/ml. The lysates were centrifuged at 16,000 × *g* for 15 min. The supernatants were collected and used for IgM-detection ELISA.

Lungs were mixed with lysis buffer and homogenized by shaking with a zirconium bead at 30 times/s for 3 min using a mixer mill (MM300; Retsch, Haan, Germany). The homogenates were kept on ice for 30 min and centrifuged at 6000 × *g* for 10 min. Supernatants were collected and used for viral antigen detection.

2.7. IgM-ELISA

Plates were coated with 50 μl of rabbit IgG against hamster IgM μ chain (diluted to 25 μg/ml in PBS; Rockland Immunochemicals, Gilbertsville, PA, USA) at 4 °C overnight. The plates were blocked with 200 μl of 3% BSA in PBS at 37 °C for 1 h. The plates were washed three times with PBST, and 50 μl of each serum sample diluted to 1:100 was added and incubated at 37 °C for 1 h. After washing, 50 μl of each cell lysate diluted to 1:10 with PBST was added to each well. The plates were then incubated at 37 °C for 1 h and washed. The biotinylated monoclonal antibody E5/G6 diluted to 1 μg/ml with PBST was added and incubated at 37 °C for 1 h. The plates were then washed, and 50 μl of peroxidase conjugated NeutrAvidin™ (Pierce Biotechnology, Inc., Rockford, IL, USA) diluted to 1 μg/ml with PBST

was added. After 1 h of incubation at 37 °C followed by washing, 100 μl of *o*-phenylenediamine substrate with hydrogen peroxide was added, and the plates were incubated at 37 °C for 30 min. The absorbance was measured at 450 nm, and the value for each serum sample was calculated by subtracting the absorbance of the well with uninfected Vero E6 cell lysate from that of the corresponding well with PUUV-infected cell lysate.

2.8. Focus reduction neutralization test (FRNT)

The neutralizing antibody was assessed by a focus reduction neutralization test. Heat-inactivated (56 °C, 30 min) serum samples from PUUV-infected hamsters were serially diluted in EMEM and then mixed with an equal volume of EMEM containing approximately 100 FFU of PUUV. This mixture was incubated at 37 °C for 1 h, and then 50 μl of the mixture was added to confluent Vero E6 cells grown in 96-well plates. After 1 h of incubation at 37 °C, the mixture was removed and the cells were overlaid with EMEM containing 1.5% carboxymethyl cellulose. After incubation at 37 °C for 10 days, the overlay medium was removed and cells were washed with PBS. The cells were then fixed with methanol for 15 min at room temperature. The viral foci were stained with E5/G6 (0.5 μg/ml) and Alexa Fluor® 555-conjugated anti-mouse IgG (1:1000; Invitrogen). The neutralizing antibody titer of each serum sample was determined as the reciprocal of the maximum dilution of the serum that reduced the number of foci by 80% or more as compared to the control samples.

2.9. N-ELISA

The 96-well plates were coated with 50 μl per well of MAb E5/G6 diluted to 2 μg/ml in PBS. After overnight incubation at 4 °C, 200 μl of 3% BSA in PBS was added for blocking; the plates were incubated at 37 °C for 1 h and then washed. After the addition of 50 μl of lung homogenates to each well, the plates were incubated at 37 °C for 1 h. After washing the plates, 50 μl the biotinylated MAb E5/G6 diluted to 1 μg/ml with PBST was added to each well. After 1 h of incubation at 37 °C and washing, 50 μl of peroxidase conjugated NeutrAvidin™ diluted to 1 μg/ml with PBST was added and incubated at 37 °C for 1 h. After washing, 100 μl of *o*-phenylenediamine substrate with hydrogen peroxide was added to each well. The plates were incubated at 37 °C for 30 min and the absorbance was read at 450 nm.

2.10. RNA extraction

Total RNA was extracted from tissues (brain, heart, lung, liver, spleen, and kidney) using ISOGEN (Nippon Gene Co., Ltd., Tokyo, Japan) according to the manufacturer's protocol. Extracted RNA was dissolved in 50 μl of deionized, diethylpyrocarbonate (DEPC)-treated water. RNA was then treated with DNase. The reaction for DNase treatment was carried out in a total volume of 50 μl containing 15 μg of RNA, 5 μl of 10 × DNase buffer, 10 U of DNase I (Takara Bio Inc., Otsu, Japan), and 20 U of RNase Out ribonuclease inhibitor (Invitrogen). The mixtures were incubated at 37 °C for 30 min. Total RNA was then purified by lithium chloride and dissolved in 30 μl of DEPC-treated water.

2.11. Reverse transcription (RT)

A 20-μl reaction mixture containing 5 μg of RNA, 0.75 μg of random primers, and 0.5 mM dNTP was incubated in a thermocycler at 70 °C for 10 min, 25 °C for 10 min, and chilled on ice for 3 min. After the addition of 10 μl of a mixture including 6 μl of 5 × first-strand buffer, 10 μM DTT, and 200 U of Superscript™ II reverse transcriptase (Invitrogen), the reactions were incubated at 42 °C for 50 min and heated at 70 °C for 15 min. Thereafter, the mixture was used as the cDNA sample.

2.12. Polymerase chain reaction (PCR)

The S segment of the PUUV genome was amplified by PCR in a 25-μl reaction mixture containing 1 μl of cDNA, 2.5 μl of 10 × HIFI buffer, 2 mM $MgSO_4$, 0.2 mM dNTP, 0.2 μM forward primer SotS172Fw (5′-CTG CAA GCC AGG CAA CAA ACA GTG TCA GCA-3′), 0.2 μM reverse primer SotS894Rv (5′-GTC TGC CAC ATG ATT TTT GTC AAG CAC ATC-3′), and 1.25 U of Platinum® *Taq* DNA Polymerase High Fidelity (Invitrogen). Thermal cycling consisted of heating at 94 °C for 2 min followed by 35 cycles at 94 °C for 30 s, 60 °C for 30 s, and 68 °C for 2 min. The amplified products were electrophoresed in a 1% agarose gel, stained with ethidium bromide, and examined for bands of the appropriate size. Similarly, the PCR products were further amplified using inner primers, SotS269Fw (5′-CTA AAC CTA CTG ACC CGA CTG G-3′) and SotS707Rv (5′-GAC CCC CAT AAC TGG ACT CAT-3′). The incubation conditions for the secondary reaction consisted of heating at 94 °C for 2 min and 35 cycles at 94 °C for 30 s, 57.5 °C for 30 s, and 68 °C for 2 min.

2.13. Quantitative real-time PCR

Each cDNA sample from various organs of infected hamsters was tested in quadruplicate. Each 25-μl reaction mixture contained 2.5 μl of cDNA, 12.5 μl of TaqMan® Universal PCR Master Mix (Applied Biosystems, Carlsbad, CA, USA), 0.9 μM forward primer Sotkamo62Fw (5′-TCC AAG AGG ATA TAA CCC GCC AT-3′), 0.9 μM reverse primer Sotkamo257Rv (5′-TTC CTG GAC ACA GCA TCT GC-3′), and 0.2 μM fluorescent probe Sotkamo194 probe (5′-TGT CAG CAC TGG AGG A-3′). The probe was labeled with the reporter dye, 6-carboxyfluorescein (FAM) at the 5′ end, and nonfluorescent quencher and minor groove enhancer (MGB) at the 3′ end. PCR cycling conditions consisted of incubations at 50 °C for 2 min and 95 °C for 10 min, followed by 60 cycles at 95 °C for 15 s and 60 °C for 1 min.

Rodent GAPDH mRNA expression was also determined in each sample. Each 25-μl reaction mixture contained 2.5 μl of cDNA, 12.5 μl of TaqMan® Universal PCR Master Mix, 0.1 μM rodent GAPDH forward and reverse primers, and 0.2 μM rodent GAPDH probe labeled with a VIC dye at the 5′ end. The levels of viral genome and GAPDH mRNA were quantified from a standard curve. The results were expressed as the ratio of the copy number of viral RNA to nanograms of GAPDH mRNA.

2.14. Histopathological and immunohistochemical analysis

Animals ($n = 2$ per group) were anesthetized and heart, lung, liver, spleen, adrenal gland, kidney, and brain samples were harvested for histopathological investigation. Tissues were fixed with 10% phosphate-buffered formalin and routinely embedded in paraffin, sectioned, and stained with hematoxylin and eosin. The Vector M.O.M. Immunodetection Kit (Vector Laboratories, Burlingame, CA, USA) was used for the detection of the PUUV antigens on paraffin-embedded sections. Antigens were retrieved by hydrolytic autoclaving for 10 min at 121 °C in 10 mM sodium citrate-sodium chloride buffer (pH 6.0). Endogenous peroxidase activity was blocked by incubation in 1% hydrogen peroxide in methanol for 30 min. The first antibody was the monoclonal antibody E5/G6 (1 μg/ml, overnight at 4 °C).

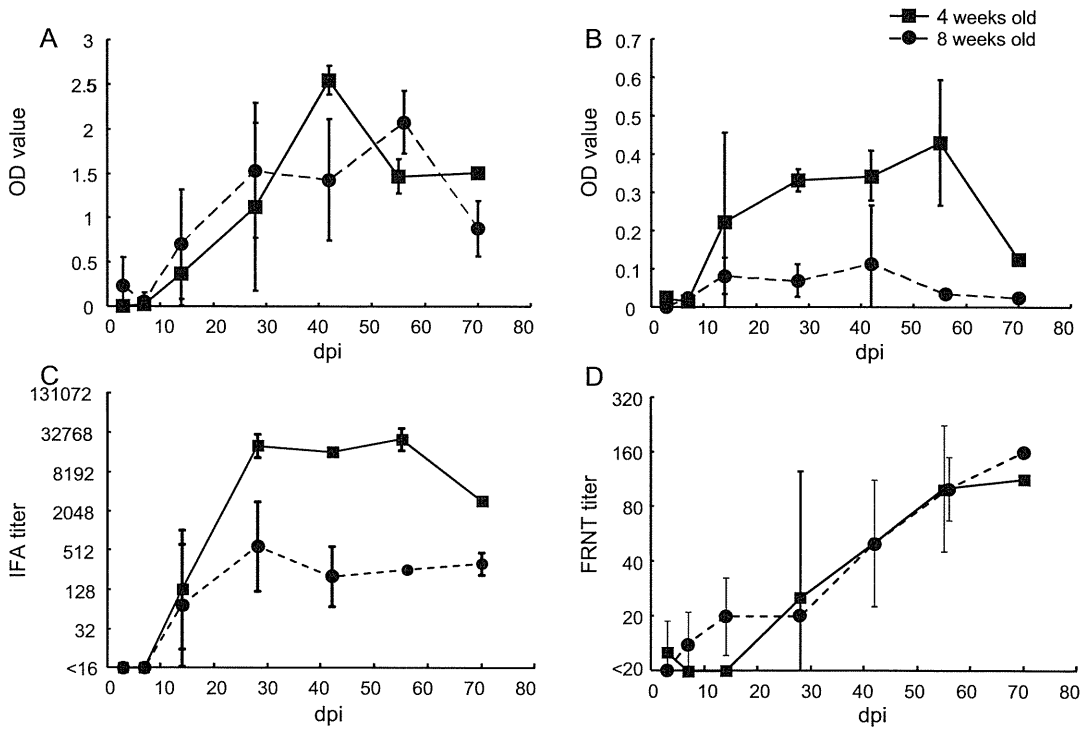

Fig. 1. Antibody responses in hamsters infected by the PUUV Sotkamo strain. Kinetics of IgG (A) and IgM (B) responses in hamsters inoculated at 4 and 8 weeks old as determined by ELISA. Kinetics of IgG responses were also determined by IFA (C). Neutralizing antibody titers of serum samples were evaluated by the 80% focus reduction method (D). Error bars represent the standard deviation.

3. Results

3.1. Body weight and clinical signs

To investigate whether PUUV causes disease in hamsters, we carefully observed clinical symptoms of the animals daily and measured their body weight. During the observation period, infected hamsters showed no signs of clinical illness or there is no difference between the transition of infected animals and that of uninfected animals (data not shown).

3.2. Antibody responses

To investigate the host response to PUUV infection, serum samples were collected at various time points from 3 to 70 dpi and analyzed for the presence of antibodies against PUUV by ELISA, IFA, and FRNT.

The serum levels of IgG and IgM antibodies against the viral N were measured by ELISA. The IgG antibody was first detectable at 14 dpi, peaked at 42 or 56 dpi, and maintained until 70 dpi in both 4- and 8-week-old hamsters (Fig. 1A). Little difference was observed between the IgG responses of hamsters inoculated at 4 and 8 weeks of age.

The IgM responses were also first detectable at 14 dpi from the sera of hamsters inoculated at 4 and 8 weeks old (Fig. 1B). The IgM responses of the hamsters inoculated at 4 weeks old increased gradually and were detectable until the end of the observation period, whereas the hamsters inoculated at 8 weeks old maintained IgM responses at quite a low level.

The results of IFA became positive at 14 dpi in 4- and 8-week-old hamsters, with titers ranging from 1:16 to 1:1024 (Fig. 1C). The IFA titers of hamsters inoculated at 4 weeks old increased greatly and reached the maximum level at 28 dpi, with titers ranging from 1:16,384 to 1:32,768. The IFA titers were maintained at the highest level for the next 4 weeks and declined at 70 dpi. In contrast, the IFA titers of hamsters inoculated at 8 weeks old reached the maximum level at 28 dpi with titers ranging from 1:128 to 1:8192 and were maintained at almost the same level until 70 dpi. The maximal titers of the hamsters inoculated at 8 weeks old were apparently lower level than those of 4-week-old hamsters.

Neutralizing antibodies were produced in both hamsters inoculated at 4 and 8 weeks old (Fig. 1D). In the serum samples of hamsters inoculated at 4 weeks old, the neutralizing antibodies were not detected from 3 to 14 dpi, but were first detectable from 28 dpi and the antibody titer increased continuously. In the serum samples of hamsters inoculated at 8 weeks old, neutralizing antibodies were detected from 7 dpi and increased gradually, as those of the 4-week-old hamsters.

3.3. Viral load in organs and blood clots

To examine the PUUV distribution in the body, organ and blood samples were collected at 3 to 70 dpi, and the PUUV load in various organs and blood clots was measured by quantitative real-time PCR. For the samples of hamsters inoculated at 4 weeks old, viral RNA was detected in various organs and blood clots (Fig. 2 and Table 1). In lung samples, viral RNA was detected from 3 dpi and peaked at 14 dpi with values ranging from 1.3×10^4 to 8.7×10^4 viral RNA copies/ng of GAPDH mRNA. Then the viral load declined gradually, but the viral RNA was maintained to 70 dpi. In kidney and spleen samples, high levels of viral RNA were also detected. Viral RNA was detected from 7 dpi and was maintained until the end of the observation period with values ranging from 9.5×10^{-1} to 2.4×10^3 and 4.3×10^0 to 9.9×10^2 viral RNA copies/ng of GAPDH mRNA from kidney and spleen samples, respectively. In liver samples, the viral RNA became positive from 7 dpi and the viral load peaked at 14 dpi with values ranging from 7.0×10^1 to 1.8×10^3 viral RNA copies/ng of GAPDH mRNA. Then the viral RNA levels declined quickly and became undetectable from 55 dpi. In heart samples, the viral RNA was detectable from 7 dpi and was maintained through 70 dpi with

Table 1
Viral load in tissues and antibody responses in sera of PUUV infected hamsters (4 weeks old).

Days post inoculation	No.	Antigen	Viral load (Real-time PCR: viral RNA copies/ng of GAPDH mRNA)							Antibody (IgG)		Antibody (IgM)	Neutralizing antibody
		N-ELISA[a]	Lung	Kidney	Spleen	Liver	Heart	Brain	Blood clot	IgG-ELISA	IFA	IgM-ELISA	FRNT
3	1	0.409	3.8×10^{-1}	–	–	–	–	–	–	0	<16	0.031	<20
	2	0.4055	1.9×10^{1}	–	–	–	–	–	2.8×10^{-1}	0	<16	0.0265	<20
	3	0.3965	1.7×10^{0}	–	–	–	–	–	–	0	<16	0.0095	20
7	4	0.435	2.1×10^{0}	–	–	–	–	–	–	0	<16	0.01	<20
	5	0.3705	1.9×10^{2}	9.5×10^{-1}	4.3×10^{0}	6.1×10^{0}	–	–	3.4×10^{-1}	0	<16	0.027	<20
	6	0.936	4.8×10^{4}	1.1×10^{3}	6.3×10^{2}	1.0×10^{3}	2.4 × 101	5.8×10^{-1}	3.9×10^{1}	0.071	<16	0.008	<20
14	7	0.391	1.3×10^{4}	5.6×10^{2}	1.6×10^{2}	7.0×10^{1}	5.8×10^{0}	9.4×10^{1}	–	0	1024	0.4925	<20
	8	2.4625	8.7×10^{4}	1.0×10^{3}	9.4×10^{2}	1.2×10^{3}	5.5×10^{1}	7.8×10^{1}	3.4×10^{1}	0.3855	16	0.084	<20
	9	2.3485	8.1×10^{4}	8.2×10^{2}	9.9×10^{2}	1.8×10^{3}	1.7×10^{1}	1.1×10^{2}	6.3×10^{1}	0.7145	128	0.0865	<20
28	10	0.5475	1.3×10^{2}	1.6×10^{1}	2.2×10^{2}	1.1×10^{0}	8.5×10^{-1}	2.4×10^{1}	–	2.211	32768	0.2995	<20
	11	0.3635	3.2×10^{2}	6.7×10^{2}	1.4×10^{2}	1.0×10^{1}	1.2×10^{1}	9.2×10^{3}	1.1×10^{2}	0.4935	16384	0.343	<20
	12	0.5165	9.4×10^{2}	8.4×10^{1}	3.7×10^{2}	1.8×10^{1}	3.2×10^{1}	3.1×10^{2}	–	0.659	16384	0.3545	160
42	13	0.513	1.8×10^{2}	1.8×10^{2}	2.7×10^{1}	2.0×10^{-1}	5.9×10^{0}	1.9×10^{1}	–	2.652	16384	0.3795	80
	14	0.4	1.2×10^{2}	2.4×10^{3}	1.6×10^{2}	–	7.8×10^{0}	1.9×10^{0}	–	2.6265	16384	0.2625	20
	15	0.3505	2.7×10^{2}	2.2×10^{1}	5.6×10^{1}	–	3.2×10^{0}	2.5×10^{1}	–	2.354	16384	0.3795	80
55	16	0.3565	6.3×10^{2}	2.6×10^{2}	1.7×10^{2}	–	2.1×10^{1}	1.2×10^{4}	–	1.665	32768	0.5855	160
	17	0.503	9.7×10^{1}	1.6×10^{1}	5.1×10^{1}	–	3.2×10^{0}	6.4×10^{1}	2.5×10^{-4}	1.47	16384	0.2605	40
	18	0.3885	4.5×10^{2}	1.9×10^{2}	7.1×10^{1}	–	6.7×10^{0}	2.0×10^{1}	–	1.2705	32768	0.4435	160
70	19	0.511	–	1.4×10^{0}	–	–	–	–	–	1.583	512	0.045	160
	20	0.4375	7.8×10^{1}	3.1×10^{2}	6.6×10^{1}	–	3.5×10^{-1}	4.0×10^{0}	1.6×10^{-2}	1.4185	16384	0.203	80

(–) Under the detectable level.
[a] Cut off value = 0.6.

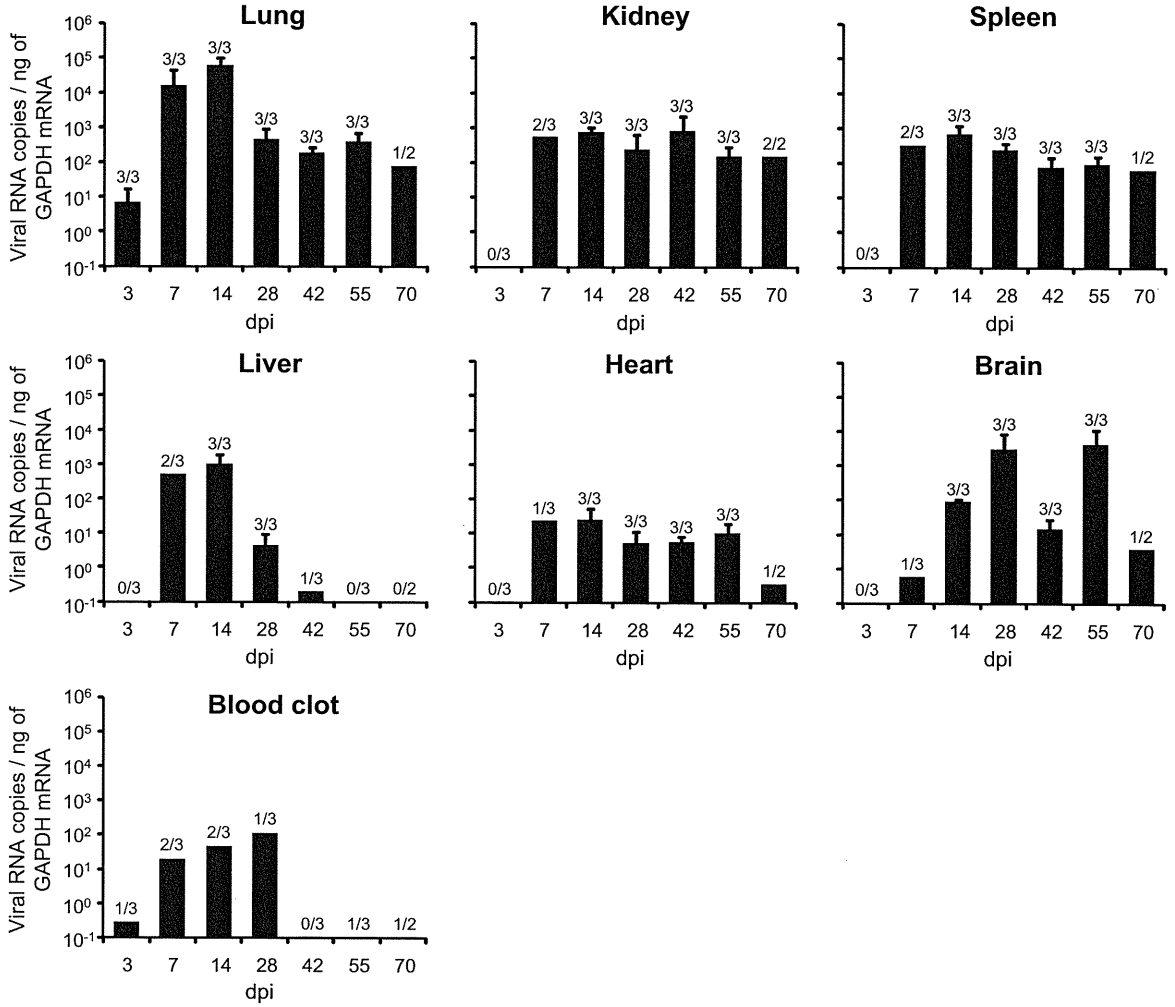

Fig. 2. Viral loads of hamsters inoculated at 4 weeks old. The viral load in each organ was measured by quantitative real-time PCR and is expressed as the mean of all positive organs at each time point. The number of positive organs/organs tested is expressed above the bar for each time point. Error bars represent the standard deviation.

values ranging from 3.5×10^{-1} to 5.5×10^{1} viral RNA copies/ng of GAPDH mRNA, but the RNA levels were lower compared to those detected in other organs such as the lung, kidney, and spleen. In brain samples, the viral RNA was detected from 7 dpi and observed through 70 days, and showed a double-peaked pattern at 28 and 55 dpi with high levels around 1.0×10^{4} viral RNA copies/ng of GAPDH mRNA. In blood clot samples, viral RNA was detected occasionally from 3 to 70 dpi, with values ranging from 2.5×10^{-4} to 6.3×10^{1} viral RNA copies/ng of GAPDH mRNA.

For the organ and blood samples of hamsters inoculated at 8 weeks old, the highest value of viral RNA was also detected in lung samples (Fig. 3 and Table 2). The viral RNA in lungs was detected from 7 to 42 dpi, ranging from 3.0×10^{-1} to 8.9×10^{3} viral RNA copies/ng of GAPDH mRNA, and then became undetectable from 56 dpi. In kidney, spleen, liver, and heart samples, viral RNA was detected occasionally from 7 and 56 dpi. In brain samples, no viral RNA was detected at any time point of infection. No viral RNA was detected from saliva, urine, or feces (data not shown).

3.4. Antigen detection from lungs

Lung samples were analyzed for the presence of viral N. To estimate the cutoff value of N-ELISA, 20 samples of lung from uninfected hamsters were tested. A cutoff value of 0.6 was determined as the mean absorbance value of 20 uninfected hamster samples plus three times the standard deviation (data not shown).

Lungs of hamsters inoculated at 4 weeks old were tested (Table 1). Only three of 20 samples showed absorbance values greater than 0.6; one sample was taken at 7 dpi and two samples at 14 dpi. The viral RNA levels of these N-positive samples were also high, with values ranging from 4.8×10^{4} to 8.7×10^{4} copies/ng of GAPDH mRNA. Therefore, the results of N-ELISA and quantitative real-time PCR corresponded well with each other. All other samples were negative by N-ELISA.

Lungs of hamsters inoculated at 8 weeks old were also tested, but all samples were negative for hantavirus N (Table 2).

3.5. Pathological studies

To reveal whether PUUV infection in hamsters causes pathological changes, and to determine cell tropism of viral antigens in organs, we examined the organs of PUUV-infected hamsters through pathological and histochemical analyses (Figs. 4–6 and Table 3).

Lung, kidney, spleen, liver, heart, brain, and adrenal gland were stained with hematoxylin and eosin for morphological study and with monoclonal antibody against hantaviral N to determine the presence of viral proteins.

Histopathological changes and hantavirus-specific staining were observed in some organs of hamsters inoculated at 4 weeks old. At 7 dpi, thickened alveolar wall was observed with very slight cellular infiltration of neutrophils and mononuclear cells (Fig. 4A).

Table 2
Viral load in tissues and antibody responses in sera of PUUV infected hamsters (8 weeks old).

Days post inoculation	No.	Antigen	Viral load (Real-time PCR: viral RNA copies/ng of GAPDH mRNA)						Antibody (IgG)		Antibody (IgM)	Neutralizing antibody
		N-ELISA[a]	Lung	Kidney	Spleen	Liver	Heart	Brain	IgG-ELISA	IFA	IgM-ELISA	FRNT
3	1	0.3605	–	–	–	–	–	–	0.5945	<16	0	<20
	2	0.4185	–	–	–	–	–	–	0	<16	0.001	<20
	3	0.4	–	–	–	–	–	–	0.102	<16	0	<20
7	4	0.4115	4.0×10^{1}	–	–	1.2×10^{0}	–	–	0	<16	0.013	<20
	5	0.479	8.9×10^{3}	1.0×10^{2}	2.8×10^{2}	1.9×10^{2}	1.0×10^{1}	–	0	<16	0.0325	<20
	6	0.398	9.3×10^{2}	N.D.[b]	N.D.	N.D.	N.D.	N.D.	0	<16	0.0265	20
	7	0.295	5.7×10^{1}	–	6.0×10^{0}	1.3×10^{0}	–	–	0.205	<16	0.0115	20
14	8	N.D.	N.D.	N.D.	N.D.	N.D.	N.D.	N.D.	0.591	128	0.128	40
	9	N.D.	N.D.	N.D.	N.D.	N.D.	N.D.	N.D.	0.626	256	0.097	20
	10	0.427	2.5×10^{3}	4.9×10^{1}	7.1×10^{1}	2.0×10^{1}	1.6×10^{0}	–	0.3775	<16	0.031	20
	11	0.3475	–	1.3×10^{-1}	–	–	–	–	0.1685	<16	0.03	<20
	12	0.398	1.4×10^{2}	4.3×10^{-1}	–	–	–	–	1.7535	1024	0.1215	20
28	13	N.D.	N.D.	N.D.	N.D.	N.D.	N.D.	N.D.	1.7935	8192	0.121	20
	14	0.53	N.D.	N.D.	N.D.	N.D.	N.D.	N.D.	1.9575	512	0.027	20
	15	0.4605	3.0×10^{-1}	–	–	–	–	–	1.551	256	0.0305	20
	16	0.2315	9.9×10^{1}	–	–	–	–	–	2.1175	512	0.062	20
	17	0.3535	3.4×10^{1}	–	–	–	–	–	0.2285	128	0.1035	20
42	18	0.404	1.5×10^{2}	1.9×10^{1}	1.1×10^{1}	–	6.4×10^{-1}	–	1.6105	512	0.2905	80
	19	0.394	–	–	–	–	–	–	1.9955	256	0.0155	80
	20	0.3935	–	–	–	–	–	–	0.6655	64	0.027	20
56	21	0.4315	–	–	4.5×10^{0}	–	–	–	2.2365	256	0.0255	160
	22	0.3965	–	–	–	–	–	–	1.6765	256	0.0285	80
	23	0.3075	–	–	–	–	–	–	2.3095	256	0.0515	80
70	24	0.348	–	–	–	–	–	–	0.531	256	0.0145	160
	25	0.4345	–	–	–	–	–	–	1.1515	256	0.0375	160
	26	0.404	–	–	–	–	–	–	0.943	512	0.019	160

(–) Under the detectable level.
[a] Cut off value = 0.6.
[b] Not done.

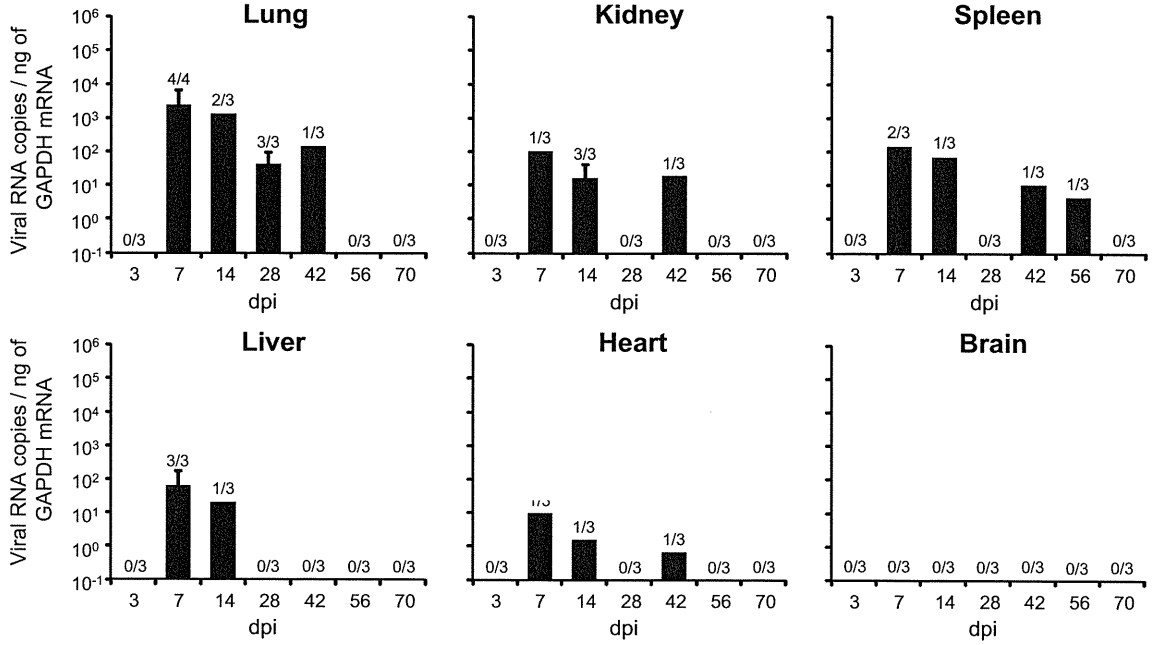

Fig. 3. Viral loads of hamsters inoculated at 8 weeks old. The viral load in each organ was measured by quantitative real-time PCR and is expressed as the mean of all positive organs at each time point. The number of positive organs/organs tested is expressed above the bar for each time point. Error bars represent the standard deviation.

Upon immunohistochemical analysis, viral antigens were localized in those pulmonary cells (Fig. 4B). At 14 dpi, cellular infiltrations including multinuclear giant cells were detected in the alveolar area (Fig. 4C), and hantavirus antigen-positive cells were detected in these cells (Fig. 4D). At 28 and 56 dpi, no detectable histopathological changes and viral antigens were observed (Fig. 4E and F).

The kidneys of infected hamsters showed no clear histopathological changes. By immunohistochemical analysis, viral antigens were found in cells of the kidney medulla from 7 and 14 dpi (Fig. 5A and B). At 28 and 56 dpi, tubular epithelial cells and vascular endothelial cells of the renal pelvis were PUUV-positive (Fig. 5C and D).

In the adrenal glands, very slight vacuolar degeneration was observed in hantavirus antigen-positive cells in the adrenal cortex of the hamster at 7 dpi (Fig. 5E). At 14 dpi, slight inflammatory infiltration and virus antigen-positive cells were observed in the adrenal cortex (Fig. 5F). In adrenal glands at 28 and 56 dpi, degenerated cells were present and virus antigens were positive in the nuclei (data not shown).

At 7 dpi, histopathological changes were absent in the brain of infected hamsters. Also, hantavirus-specific staining was not observed in the brain. At 14 dpi, slight cell infiltrations with mononuclear cells and microglia were detected in the cortex of the cerebellum from one of the infected hamsters (Fig. 6A). Upon immunohistochemical analysis, virus antigen was observed in degenerated Purkinje cells at 14 dpi (Fig. 6B). At 28 dpi, slight cell infiltrations were seen in the third ventricle (Fig. 6C), and ependymal cells were PUUV- positive (Fig. 6D).

In addition to these organs, we also examined the spleens, livers, hearts, and cerebrums. No histopathological changes or hantavirus-specific staining were found (data not shown).

In contrast to the organs of hamsters inoculated at 4 weeks old, those of hamsters inoculated at 8 weeks old showed no histopathological changes or hantavirus specific staining (data not shown).

Table 3
Detection of PUUV antigen from tissues of infected hamsters by immunohistochemical analysis.

Age	Tissue	No. of virus-positive/no. of tested animals				
		7 dpi	14 dpi	28 dpi	56 dpi	mock
4	Lung	1/1	2/2	0/2	0/2	0/1
	Kidney	1/1	2/2	2/2	2/2	0/1
	Spleen	0/1	0/2	0/2	0/2	0/1
	Liver	0/1	0/2	0/2	0/2	0/1
	Heart	0/1	0/2	0/2	0/2	0/1
	Cerebrum	0/1	0/2	0/2	0/2	0/1
	Cerebellum	0/1	1/2	1/2	0/2	0/1
	Adrenal gland	1/1	2/2	1/2	1/2	NE
8	Lung	0/1	0/2	0/2	NE	0/1
	Kidney	0/1	0/2	0/2	NE	0/1
	Spleen	0/1	0/2	0/2	NE	0/1
	Liver	0/1	0/2	0/2	NE	0/1
	Heart	0/1	0/2	0/2	NE	0/1
	Cerebrum	0/1	0/2	0/2	NE	0/1
	Cerebellum	NE	0/1	0/1	NE	0/1
	Adrenal gland	NE	NE	NE	NE	NE

NE, not examined.

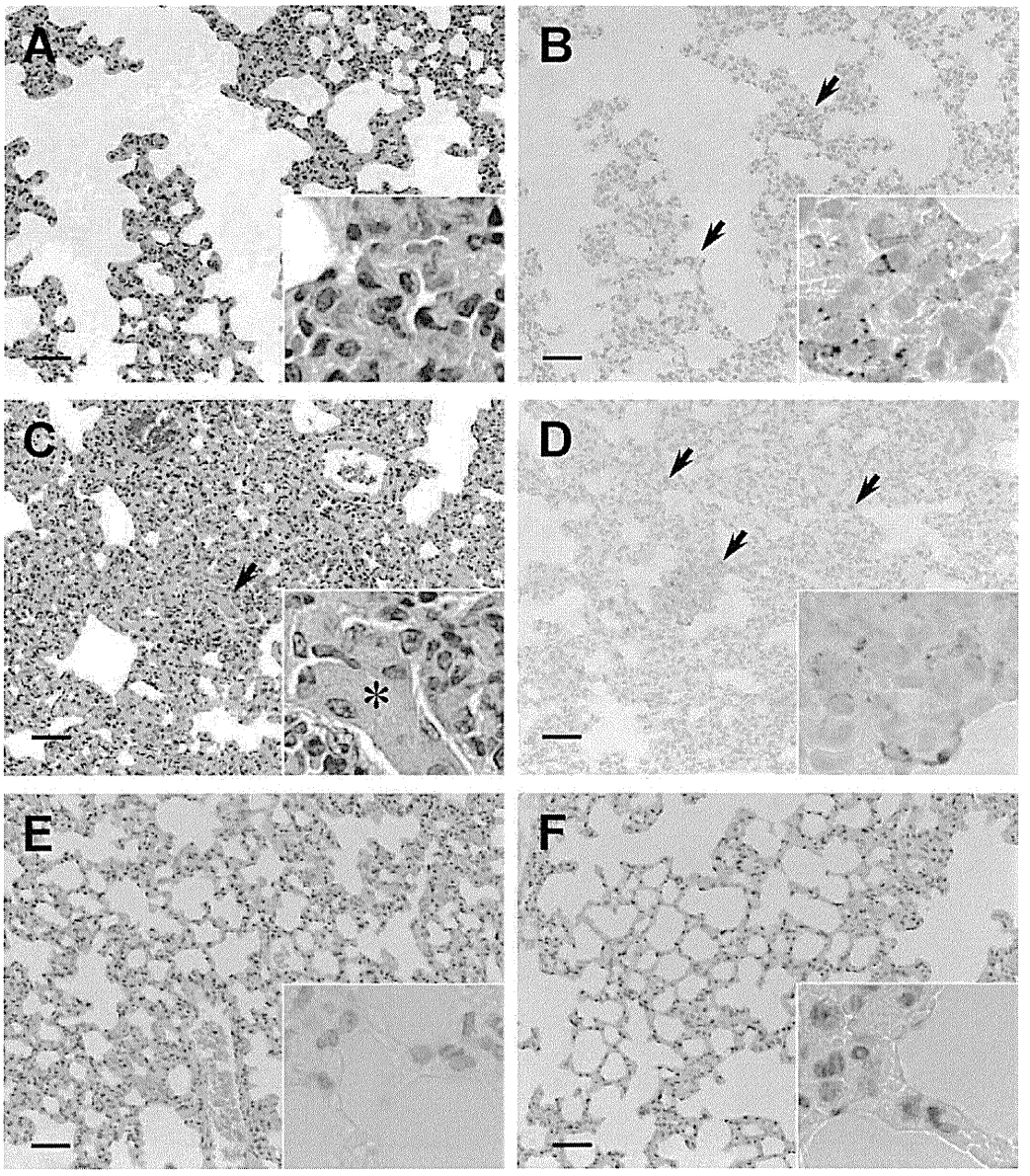

Fig. 4. Morphologic and immunohistochemical examination of lungs from hamsters inoculated at 4 weeks old. Bar, 50 μm. (A) Very slight cellular proliferation of neutrophils and mononuclear cells were observed in the interstitium at 7 dpi. (B) Immunohistochemical staining with hantavirus-specific antibody revealed virus antigen-positive cells (arrows) in the cellular proliferation sites in the alveolar area at 7 dpi. (C) Cellular infiltrations including macrophages and multinuclear giant cells (arrow, inset, asterisk) in the alveolar area at 14 dpi. (D) PUUV-positive cells (arrows) in the alveolar area at 14 dpi. (E, F) No histopathological change and viral antigen were observed at 28 dpi (E) and 56 dpi (F).

4. Discussion

Although many researchers have reported experimental infections using various animal species with several hantaviruses, few reliable animal models of hantavirus infection exist. As a disease model for HCPS, a previous study showed that ANDV, a causative agent of HCPS in South America, causes a lethal disease in Syrian hamsters, of which the characteristics were very similar to HCPS in humans (Hooper et al., 2001). Maporal virus, a South American hantavirus, also causes a disease in Syrian hamsters that resembles HCPS closely (Milazzo et al., 2002). In addition, Cynomolgus macaques infected with PUUV, which causes a mild form of HFRS, has been reported as a disease model for HFRS (Klingström et al., 2002). In contrast to the animal models of human infection, an animal model of persistent infection that mimics the infection of natural rodent reservoirs had not been established. To date, newborn animals infected with hantavirus experimentally were reported to show persistent infection (Araki et al., 2003; Compton et al., 2004; Kariwa et al., 1996; Tanishita et al., 1986). However, maternal antibodies are believed to protect newborn animals from vertical transmission (Bernshtein et al., 1999; Borucki et al., 2000; Botten et al., 2002; Gavrilovskaya et al., 1990; Taruishi et al., 2008). Therefore, in nature, hantavirus infection is believed to occur in adults. Herein, we report that PUUV in Syrian hamsters inoculated as subadults shows persistent infection that is similar to that in its principal rodent host, the bank vole (*M. glareolus*).

In this study, we demonstrated that the organs of Syrian hamsters infected with PUUV at 4 weeks old contained a high amount of viral RNA that was maintained for at least 70 days. Most organs showed the peak of viral RNA copies from 7 to 14 dpi followed by a gradual decline. In addition, the viral RNA was maintained for at least 70 days despite the existence of neutralizing antibodies. These data correspond well with the results of previous studies conducted on experimentally infected host rodents (Botten et al.,

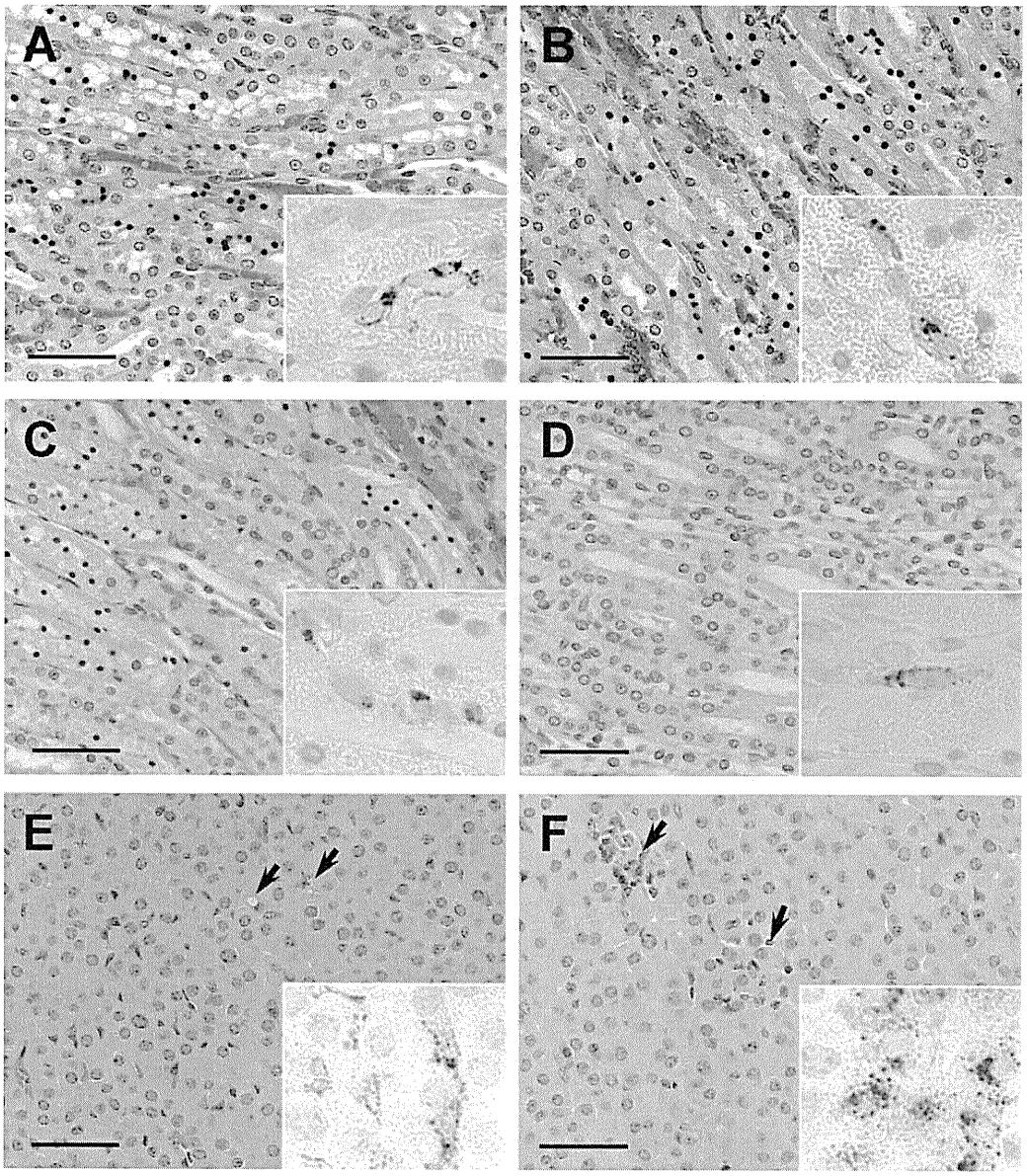

Fig. 5. Morphologic and immunohistochemical examination of kidneys and adrenal glands from hamsters inoculated at 4 weeks old. Bar, 50 μm. (A, B) PUUV-positive cells were detected in the kidney medulla of the hamsters at 7 dpi (A) and 14 dpi (B). (C, D) PUUV-positive cells were tubular epithelial cells and vascular endothelial cells of the renal pelvis at 28 dpi (C) and 56 dpi (D). (E) At 7 dpi, very slight vacuolar degeneration cells (arrows) present in the adrenal cortex were positive for virus antigen (inset). (F) Slight inflammatory infiltrations (arrows) and virus antigen-positive cells (inset) in the adrenal cortex at 14 dpi.

2000; Hutchinson et al., 1998). Therefore, our findings suggest that PUUV in Syrian hamsters establishes persistent infection similar to that in the natural rodent reservoir.

For most individuals, the highest titer of viral RNA was detected in lung samples. In particular, lung samples at 7 and 14 dpi from hamsters inoculated at 4 weeks old contained high copies of viral RNA. By N-ELISA, the antigens were also detected in these samples. These data suggest that the lung is a suitable site for viral replication. Additionally, kidney, spleen, and brain samples also showed high copy numbers of RNA. This virus distribution pattern resembles the results of studies on experimental infection with PUUV in *M. glareolus* (Yanagihara et al., 1985), natural infection with PUUV in *M. glareolus* (Korva et al., 2009), and other hantaviruses in their rodent hosts (Botten et al., 2000; Compton et al., 2004; Daud et al., 2007; Hutchinson et al., 1998; Kariwa et al., 1996; Tanishita et al., 1986). In adrenal gland samples from hamsters inoculated at 4 weeks old, viral antigens were observed from 7 to 56 dpi. Other studies have also reported high titers of virus and high prevalence of virus in adrenal glands (Hinson et al., 2004; Hutchinson et al., 1998). These results indicate that the adrenal gland may be one of the sites of replication and maintenance of hantavirus. In liver samples from hamsters inoculated at 4 weeks old, the titer of viral RNA at 7 and 14 dpi was high like in other organs, but viral RNA was transient unlike in other organs. Similar results were also obtained in several studies (Compton et al., 2004; Fulhorst et al., 2002; Hutchinson et al., 1998). Viral replication in the liver may more suppressed than in other organs.

Unlike the natural rodent host (Gavrilovskaya et al., 1990; Hardestam et al., 2008; Yanagihara et al., 1985), the viral RNA was not detected from saliva, urine, or feces samples of hamsters with PUUV. The amount of excreted PUUV from infected hamsters may be extremely low level. Another possible explanation is that the virus shedding pattern of PUUV-infected hamster may be intermittent or transient like SNV-infected deer mouse (Botten et al., 2000). To clarify this point, further study focusing on virus shedding is needed.

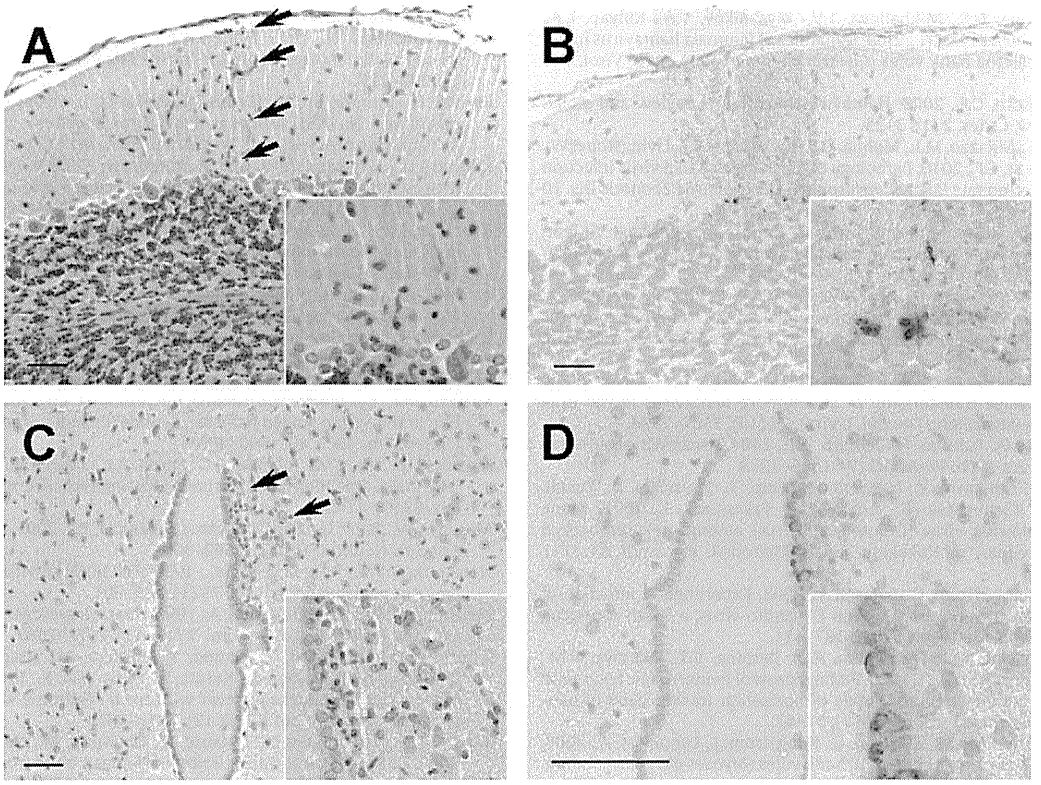

Fig. 6. Morphologic and immunohistochemical examination of brains from hamsters inoculated at 4 weeks old. Bar, 50 μm. (A) Mild cell infiltrations with mononuclear cells and microglia in the cortex of cerebellum at 14 dpi (arrows, inset) from one hamster. (B) Immunohistochemical staining with anti-hantavirus-specific antibody revealed virus antigen-positive cells in the Purkinje cell layer (inset). (C) Slight cell infiltrations around the third ventricle at 28 dpi (arrows). (D) Virus antigen-positive cells included ependymal cells at 28 dpi (inset).

It is generally believed that hantavirus infection in the natural hosts does not show apparent clinical manifestations. In this study, hamsters with PUUV showed no signs of clinical illness or loss of body weight. When hamsters were inoculated at 4 weeks old, very slight inflammatory reactions were observed in the lung, cerebellum, and adrenal gland in the acute phase of infection. These histopathological findings were different from the results of *M. glareolus* infected with PUUV, which showed that organs contained viral antigens without pathological change (Yanagihara et al., 1985); however, endothelial hyperplasia in vascular walls and lymphohistiocytic infiltration has been observed in *M. glareolus* experimentally infected with PUUV (Gavrilovskaya et al., 1990). Recent study also showed that BCCV in experimentally infected in *Sigmodon hispidus*, the principal host of BCCV, causes pneumonitis and the severity of pneumonitis is dependent on inoculated dose as well as infection period (Billings et al., 2010). Furthermore, some reports indicated that New World hantavirus in wild rodents causes pathological changes in tissues (Lyubsky et al., 1996; Netski et al., 1999). Certain level of pathological change may occur in hantavirus infection in the natural host. Because histopathological studies on natural rodent hosts infected with hantavirus are scarce, analyzing in greater detail the pathology and cell tropism of hantavirus in wild rodents is necessary.

In this study, the modes of infection differed between hamsters inoculated at 4 and 8 weeks old. Infection at 4 weeks old showed high titers of viral RNA and continued through at least 70 dpi, whereas infection at 8 weeks old was transient. IgM of hamsters inoculated at 4 weeks old was induced persistently, but that of the 8-week-old hamsters was quite low. These data suggest that 4-week-old hamsters may allow more PUUV replication to stimulate the host immune system persistently compared to 8-week-old hamsters. Hamsters infected with other viruses also showed different modes of infection between 4 and 8 weeks old (Morrey et al., 2004; Xiao et al., 2001). Therefore, the age at infection is probably an important factor in determining the mode of viral infection. At 4 weeks old, the host immune system of hamsters may still be immature, causing persistent infection in those hamsters.

In this study, Syrian hamsters infected with PUUV at 4 weeks old showed persistent infection despite the presence of neutralizing antibodies, without any clinical symptoms, which is quite similar to the infection in natural host rodents. These data indicated that hamsters could be a suitable animal model for studying hantavirus infection in the reservoir host. This animal model would be a useful tool to clarify the mechanism of persistent infection in the natural rodent reservoir. In addition, because there is few appropriate laboratory animal model for PUUV infection, this model could also be useful for *in vivo* evaluations of vaccines and antiviral therapies for the treatment of PUUV infection.

Acknowledgements

This work was supported financially by Grants-in-Aid for Scientific Research (16405034 and 17255009) from the Japanese Ministry of Education, Culture, Sports, Science and Technology, and by a Health and Labour Sciences Research Grant on Emerging and Re-emerging Infectious Diseases from the Japanese Ministry of Health, Labour and Welfare. This work was also supported by the global COE Program for Zoonosis Control (Hokkaido University).

References

Araki, K., Yoshimatsu, K., Lee, B.H., Kariwa, H., Takashima, I., Arikawa, J., 2003. Hantavirus-specific CD8(+)-T-cell responses in newborn mice persistently infected with Hantaan virus. J. Virol. 77 (15), 8408–8417.

Bernshtein, A.D., Apekina, N.S., Mikhailova, T.V., Myasnikov, Y.A., Khlyap, L.A., Korotkov, Y.S., Gavrilovskaya, I.N., 1999. Dynamics of Puumala hantavirus infection in naturally infected bank voles (*Clethrinomys glareolus*). Arch. Virol. 144 (12), 2415–2428.

Bi, Z., Formenty, P.B., Roth, C.E., 2008. Hantavirus infection: a review and global update. J. Infect. Dev. Ctries. 2 (1), 3–23.

Billings, A.N., Rollin, P.E., Milazzo, M.L., Molina, C.P., Eyzaguirre, E.J., Livingstone, W., Ksiazek, T.G., Fulhorst, C.F., 2010. Pathology of Black Creek Canal virus infection in juvenile hispid cotton rats (*Sigmodon hispidus*). Vector Borne Zoonotic Dis. 10 (6), 621–628.

Borucki, M.K., Boone, J.D., Rowe, J.E., Bohlman, M.C., Kuhn, E.A., DeBaca, R., St Jeor, S.C., 2000. Role of maternal antibody in natural infection of *Peromyscus maniculatus* with Sin Nombre virus. J. Virol. 74 (5), 2426–2429.

Botten, J., Mirowsky, K., Kusewitt, D., Bharadwaj, M., Yee, J., Ricci, R., Feddersen, R.M., Hjelle, B., 2000. Experimental infection model for Sin Nombre hantavirus in the deer mouse (*Peromyscus maniculatus*). Proc. Natl. Acad. Sci. U. S. A. 97 (19), 10578–10583.

Botten, J., Mirowsky, K., Ye, C., Gottlieb, K., Saavedra, M., Ponce, L., Hjelle, B., 2002. Shedding and intracage transmission of Sin Nombre hantavirus in the deer mouse (*Peromyscus maniculatus*) model. J. Virol. 76 (15), 7587–7594.

Compton, S.R., Jacoby, R.O., Paturzo, F.X., Smith, A.L., 2004. Persistent Seoul virus infection in Lewis rats. Arch. Virol. 149 (7), 1325–1339.

Daud, N.H., Kariwa, H., Tanikawa, Y., Nakamura, I., Seto, T., Miyashita, D., Yoshii, K., Nakauchi, M., Yoshimatsu, K., Arikawa, J., Takashima, I., 2007. Mode of infection of Hokkaido virus (Genus *Hantavirus*) among grey red-backed voles, *Myodes rufocanus*, in Hokkaido, Japan. Microbiol. Immunol. 51 (11), 1081–1090.

Fulhorst, C.F., Milazzo, M.L., Duno, G., Salas, R.A., 2002. Experimental infection of the *Sigmodon alstoni* cotton rat with Cano Delgadito virus, a South American hantavirus. Am. J. Trop. Med. Hyg. 67 (1), 107–111.

Gavrilovskaya, I.N., Apekina, N.S., Bernshtein, A.D., Demina, V.T., Okulova, N.M., Myasnikov, Y.A., Chumakov, M.P., 1990. Pathogenesis of hemorrhagic fever with renal syndrome virus infection and mode of horizontal transmission of hantavirus in bank voles. Arch. Virol. (Suppl 1), 57–62.

Hardestam, J., Karlsson, M., Falk, K.I., Olsson, G., Klingstrom, J., Lundkvist, A., 2008. Puumala hantavirus excretion kinetics in bank voles (*Myodes glareolus*). Emerg. Infect. Dis. 14 (8), 1209–1215.

Hinson, E.R., Shone, S.M., Zink, M.C., Glass, G.E., Klein, S.L., 2004. Wounding: the primary mode of Seoul virus transmission among male Norway rats. Am. J. Trop. Med. Hyg. 70 (3), 310–317.

Hooper, J.W., Larsen, T., Custer, D.M., Schmaljohn, C.S., 2001. A lethal disease model for hantavirus pulmonary syndrome. Virology 289 (1), 6–14.

Hutchinson, K.L., Rollin, P.E., Peters, C.J., 1998. Pathogenesis of a North American hantavirus, Black Creek Canal virus, in experimentally infected Sigmodon hispidus. Am. J. Trop. Med. Hyg. 59 (1), 58–65.

Jonsson, C.B., Figueiredo, L.T., Vapalahti, O., 2010. A global perspective on hantavirus ecology, epidemiology, and disease. Clin. Microbiol. Rev. 23 (2), 412–441.

Kanerva, M., Mustonen, J., Vaheri, A., 1998. Pathogenesis of puumala and other hantavirus infections. Rev. Med. Virol. 8 (2), 67–86.

Kariwa, H., Yoshizumi, S., Arikawa, J., Yoshimatsu, K., Takahashi, K., Takashima, I., Hashimoto, N., 1995. Evidence for the existence of Puumala-related virus among *Clethrionomys rufocanus* in Hokkaido,Japan. Am. J. Trop. Med. Hyg. 53 (2), 222–227.

Kariwa, H., Kimura, M., Yoshizumi, S., Arikawa, J., Yoshimatsu, K., Takashima, I., Hashimoto, N., 1996. Modes of Seoul virus infections: persistency in newborn rats and transiency in adult rats. Arch. Virol. 141 (12), 2327–2338.

Klingström, J., Plyusnin, A., Vaheri, A., Lundkvist, A., 2002. Wild-type Puumala hantavirus infection induces cytokines, C-reactive protein, creatinine, and nitric oxide in cynomolgus macaques. J. Virol. 76 (1), 444–449.

Korva, M., Duh, D., Saksida, A., Trilar, T., Avsic-Zupanc, T., 2009. The hantaviral load in tissues of naturally infected rodents. Microbes Infect. 11 (3), 344–351.

Lee, H.W., Lee, P.W., Baek, L.J., Song, C.K., Seong, I.W., 1981. Intraspecific transmission of Hantaan virus, etiologic agent of Korean hemorrhagic fever, in the rodent *Apodemus agrarius*. Am. J. Trop. Med. Hyg. 30 (5), 1106–1112.

Lyubsky, S., Gavrilovskaya, I., Luft, B., Mackow, E., 1996. Histopathology of *Peromyscus leucopus* naturally infected with pathogenic NY-1 hantaviruses: pathologic markers of HPS viral infection in mice. Lab. Invest. 74 (3), 627–633.

Milazzo, M.L., Eyzaguirre, E.J., Molina, C.P., Fulhorst, C.F., 2002. Maporal viral infection in the Syrian golden hamster: a model of hantavirus pulmonary syndrome. J. Infect. Dis. 186 (10), 1390–1395.

Morrey, J.D., Day, C.W., Julander, J.G., Olsen, A.L., Sidwell, R.W., Cheney, C.D., Blatt, L.M., 2004. Modeling hamsters for evaluating West Nile virus therapies. Antiviral Res. 63 (1), 41–50.

Muranyi, W., Bahr, U., Zeier, M., van der Woude, F.J., 2005. Hantavirus infection. J. Am. Soc. Nephrol. 16 (12), 3669–3679.

Netski, D., Thran, B.H., St Jeor, S.C., 1999. Sin Nombre virus pathogenesis in *Peromyscus maniculatus*. J. Virol. 73 (1), 585–591.

Plyusnin, A., Vapalahti, O., Vaheri, A., 1996. Hantaviruses: genome structure, expression and evolution. J. Gen. Virol. 77 (Pt 11), 2677–2687.

Tanishita, O., Takahashi, Y., Okuno, Y., Tamura, M., Asada, H., Dantas Jr., J.R., Yamanouchi, T., Domae, K., Kurata, T., Yamanishi, K., 1986. Persistent infection of rats with haemorrhagic fever with renal syndrome virus and their antibody responses. J. Gen. Virol. 67 (Pt 12), 2819–2824.

Taruishi, M., Yoshimatsu, K., Hatsuse, R., Okumura, M., Nakamura, I., Arikawa, J., 2008. Lack of vertical transmission of Hantaan virus from persistently infected dam to progeny in laboratory mice. Arch. Virol. 153 (8), 1605–1609.

Vapalahti, O., Mustonen, J., Lundkvist, A., Henttonen, H., Plyusnin, A., Vaheri, A., 2003. Hantavirus infections in Europe. Lancet Infect. Dis. 3 (10), 653–661.

Xiao, S.Y., Zhang, H., Guzman, H., Tesh, R.B., 2001. Experimental yellow fever virus infection in the Golden hamster (*Mesocricetus auratus*) II. Pathology. J. Infect. Dis. 183 (10), 1437–1444.

Yanagihara, R., Amyx, H.L., Gajdusek, D.C., 1985. Experimental infection with Puumala virus, the etiologic agent of nephropathia epidemica, in bank voles (*Clethrionomys glareolus*). J. Virol. 55 (1), 34–38.

Yoshimatsu, K., Arikawa, J., Tamura, M., Yoshida, R., Lundkvist, A., Niklasson, B., Kariwa, H., Azuma, I., 1996. Characterization of the nucleocapsid protein of Hantaan virus strain 76-118 using monoclonal antibodies. J. Gen. Virol. 77 (Pt 4), 695–704.

Glycosylation of the Envelope Protein of West Nile Virus Affects Its Replication in Chicks

Author(s) :Masashi Totani, Kentaro Yoshii, Hiroaki Kariwa, and Ikuo Takashima
Source: Avian Diseases, 55(4):561-568. 2011.
Published By: American Association of Avian Pathologists
DOI:
URL: http://www.bioone.org/doi/full/10.1637/9743-032811-Reg.1

AVIAN DISEASES 55:561–568, 2011

Glycosylation of the Envelope Protein of West Nile Virus Affects Its Replication in Chicks

Masashi Totani, Kentaro Yoshii,[A] Hiroaki Kariwa, and Ikuo Takashima

Laboratory of Public Health, Graduate School of Veterinary Medicine, Hokkaido University, Sapporo, Hokkaido 060-0818, Japan

Received 29 March 2011; Accepted and published ahead of print 9 June 2011

SUMMARY. Birds are important for the transmission of West Nile virus (WNV) in nature, but the significance of the potential *N*-linked glycosylation at position 154 in the WNV envelope (E) protein with regard to viral replication in young chickens has not been assessed. In this study, the effect of glycosylation of the WNV E protein on viral pathogenicity in birds was investigated using young domestic chicks. A higher viral load was detected in the blood and the peripheral organs, particularly the hearts, of 2-day-old chicks inoculated with a glycosylated WNV variant compared to those inoculated with the nonglycosylated variant. There was no significant difference in the neutralizing antibody titers and cytokine expression profiles in chickens inoculated with the glycosylated and the nonglycosylated WNV variants. In contrast, no virus was detected in the blood and the tissues of 3-wk-old chicks, although the host immune response was induced to similar levels as in the 2-day-old chicks. These data indicate the utility of young domestic chicks as an animal model of WNV infection; they also indicate that glycosylation of the E protein of WNV enhances multiplication in the blood and peripheral organs, which is associated with the strong pathogenicity of WNV in birds.

RESUMEN. La glicosilación de la proteína de la envoltura del virus del Nilo Occidental afecta a su replicación en los pollos.

Las aves son importantes para la transmisión de virus del Nilo Occidental en la naturaleza, pero no se ha evaluado la importancia de la potencial N-glicosilación en la posición 154 de la proteína E del virus en relación con la replicación viral en pollos jóvenes. En este estudio se investigó el efecto de la glicosilación de la proteína E del virus del Nilo Occidental en la patogenicidad en las aves, usando pollos domésticos jóvenes. Se detectó una mayor carga viral en la sangre y en los órganos periféricos, especialmente el corazón, de pollitos de dos días de edad inoculados con una variante glicosilada del virus en comparación con aquellas aves inoculadas con la variante no glicosilada. No hubo diferencias significativas en los títulos de anticuerpos neutralizantes y en los perfiles de expresión de citoquinas de los pollos inoculados con las variantes glicosilada y no glicosilada del virus. Por el contrario, no se detectó al virus en la sangre y en los tejidos de los pollos de 3 semanas de edad, aunque la respuesta inmune del huésped fue inducida a niveles similares a los observados en los pollos de 2 días de edad. Estos datos indican la utilidad de los pollos jóvenes domésticos como un modelo animal para estudiar la infección por el virus del Nilo Occidental, y también indican que la glicosilación de la proteína E del virus mejora la multiplicación en la sangre y en los órganos periféricos, que se asocia con una patogenicidad mayor del virus del Nilo Occidental en las aves.

Key words: West Nile virus, glycosylation, chick model, viral multiplication

Abbreviations: BHK = baby hamster kidney; CMC = carboxymethyl cellulose; C_T = threshold of cycles; DEPC = diethyl pyrocarbonate; d.p.i. = days postinoculation; E = envelope; EMEM = Eagle minimal essential medium; FCS = fetal calf serum; IFN = interferon; IL = interleukin; LITAF = lipopolysaccharide-induced TNF-α factor; LP = large plaque; NYC = New York City; PBS = phosphate-buffered saline; PFU = plaque-forming units; $PRNT_{80}$ = 80% plaque reduction neutralization test; s.c. = subcutaneously; SP = small plaque; TNF-α = tumor necrosis factor–α; TNFSF15 = tumor necrosis factor superfamily 15; WNV = West Nile virus

West Nile virus (WNV) is an RNA virus and member of the family *Flaviviridae*, genus *Flavivirus*. WNV is transmitted by mosquito bites and is maintained in an enzootic transmission cycle between mosquitoes and wild birds (9). WNV infection causes neurologic illness in humans and horses, which are accidental hosts. Until the early 1990s, WNV cases occurred sporadically in Africa, Europe, and the Middle East, and the virus was considered to have only moderate pathogenicity in birds, with a low mortality rate (9). In 1999, an outbreak of WNV occurred in and around New York City (NYC). Many wild and exotic birds died, and encephalitis in humans and horses was reported (1,14). In recent years, highly pathogenic WNV has been reported in Africa, America, Europe, and Russia, and it has become a public health concern (4). Birds play an important role in the transmission of WNV; thus, knowledge of the pathogenicity of WNV in birds is vital for the control and prevention of infections with this virus. Susceptibility to WNV varies by bird species. During the 1999 NYC outbreak, various species of birds died, including crows, flamingos, and eagles (6,11,13,31). Most deaths in wild birds have been in the order Passeriformes (crows and jays). American crows (*Corvus brachyrhynchos*; 3) and young domestic geese (*Anser anser domesticus*; 32) subsequently showed high susceptibility and mortality with a high level of viremia when infected with NYC isolates. WNV infection in wild birds causes depression, weight loss, and occasionally neurologic signs such as ataxia, tremors, and torticollis in highly susceptible species (31,32). WNV has been isolated from multiple organs, such as the brain, heart, spleen, liver, and kidney, and encephalitis and myocarditis have been reported (19,31,32,36). However, the details of the WNV pathogenicity remain unclear.

The flavivirus virion is spherical, with a 40 to 50–nm diameter, and is surrounded by a lipid envelope (E), which contains the viral membrane and E proteins. E protein is important for virus-cell interactions and serves as a major target of the host antibody response (25). The E protein of flaviviruses has either one or two potential *N*-linked glycosylation sites, and glycosylation of the E protein is associated with enhanced replication in mammalian and arthropod cells (7,24). Sequence analysis of various WNV strains has shown that recent highly pathogenic WNV isolates, such as the NYC

[A]Corresponding author. E-mail: kyoshii@vetmed.hokudai.ac.jp

Table 1. Primers used in quantitative real-time PCR.

Target	Primer sequence	Product size (bp)	Accession number	Reference
IFN-α	5′-CCAGCACCTCGAAT-3′ 5′-GGCGCTGTAATCGTTGTCT-3′	133	AB021154	Li *et al.* (16)
LITAF	5′-GTTACAGTTCAGACTGTGTATGTGC-3′ 5′-GCACCCCAGCAGGAAGAGGCCACC-3′	167	NM_204267	
TNFSF15	5′-CCTGAGTTATTCCAGCAACGCA-3′ 5′-ATCCACCAGCTTGATGTCACTAAC-3′	292	NM_001024578	Takimoto *et al.* (33)
IL-1β	5′-AGAAGCCTCGCCTGGATTCTGAGC-3′ 5′-AGATGTCGAAGGACTGTGAGCGGG-3′	272	NM_204524	
IL-6	5′-CGAGATGTGCAAGAAGTTCACCG-3′ 5′-TCACCATCTGCCGGATCGTGGCCG-3′	271	NM_204628	
IFN-γ	5′-CTCCCGATGAACGACTTGAG-3′ 5′-CTGAGACTGGCTCCTTTTCC-3′	113	NM_205149	Kano *et al.* (10)
β-actin	5′-CACAGATCATGTTTGAGACCTT-3′ 5′-CATCACAATACCAGTGGTACG-3′	101	NM_205518	De Boever *et al.* (5)

isolate, have a glycosylation site in the E protein. We isolated glycosylated and nonglycosylated variants from a NYC isolate (27) and found that the glycosylated variant was more highly pathogenic in young domestic chicks (18).

In this study, we analyzed the effect of the glycosylation of the E protein on the pathogenicity of WNV in young domestic chicks. Chicks were inoculated with either the glycosylated or nonglycosylated variant of WNV, and the viral multiplication kinetics and host immune response were evaluated. Our results indicate that glycosylation of the WNV E protein is important for viral multiplication in peripheral organs and that it is associated with the strong pathogenicity of WNV in birds.

MATERIALS AND METHODS

Cell lines and virus strains. Baby hamster kidney (BHK) cells (BHK-21, American Type Culture Collection: CCL-10) were maintained in Eagle minimal essential medium (EMEM; Nissui Pharmaceutical Co., Tokyo, Japan) supplemented with 8% fetal calf serum (FCS), 2 mM L-glutamine, and 1.5 g/L sodium bicarbonate. BHK-21 cells were grown and maintained at 37 C and 5% CO_2.

Two variants of WNV, 6–large plaque (LP) and 6–small plaque (SP), had been previously isolated from a NYC isolate, NY99-6922 (27). These variants were propagated once in the brains of suckling mice, and working stocks of the viruses were propagated once in *Aedes albopictus* (C6/36) cell cultures. Genome sequencing showed that 6-LP, but not 6-SP, contained the *N*-linked glycosylation motif (N-Y-S) at residues 154–156 in the E protein. 6-SP contained a mutation at position 156; thus, residues 154–156 were nonglycosylated (N-Y-P). The GenBank accession numbers for the sequences of the plaque-purified variants are as follows: 6-LP, AB185914; and 6-SP, AB185915.

Virus infection and sample collection. Young Boris-Brown chicks (*Gallus gallus domesticus*; Hokuren, Japan) were housed in a biosafety level–3 animal facility. All experiments were approved under the guidelines for using experimental animals at Hokkaido University. Two-day-old and 3-wk-old male chicks were inoculated subcutaneously (s.c.) in the femoral region with 100 plaque-forming units (PFU) of WNV (6-LP and 6-SP variant). The viruses were diluted in phosphate-buffered saline (PBS) containing 10% FCS (10% FCS-PBS). At 2 and 6 days postinoculation (d.p.i.), the chicks were euthanatized by sevoflurane overdose. Blood samples were collected from the heart and held at room temperature for 60 min and then at 4 C overnight. The blood samples were then centrifuged (3000 × *g*; 10 min), and the serum was removed and stored at −80 C. Tissues (brain, heart, spleen, liver, and kidney) were collected and stored at −80 C.

Viral titration. Viral loads in the working stocks and collected samples were titrated by plaque assay using BHK-21 cells. BHK-21 cell monolayers were grown in 12-well plates and inoculated with serial dilutions of the virus solutions. After adsorption for 60 min, the viral solution was aspirated and the cells were washed three times with PBS. An overlay (1 ml) consisting of EMEM containing 1.5% carboxymethyl cellulose (CMC; Wako, Osaka, Japan) and 2% FCS (CMC-EMEM) was added to the cells, and the plates were incubated at 37 C in a CO_2 incubator. The medium was aspirated after 3 days of incubation. The cells were then fixed and stained with 0.1% crystal violet and 10% formalin in PBS. After staining for 2 hr, the cells were washed and air-dried and the plaques were counted. Viral titers were calculated from the dilution that produced 10–100 plaques per well and are expressed as PFU/ml.

Quantitative real-time PCR. Total RNA was extracted from virus-infected chick samples (clot, heart, and spleen) using ISOGEN and ISOGEN-LS (Nippon Gene, Tokyo, Japan). RNA pellets were resuspended in diethyl pyrocarbonate (DEPC)–treated water (Ambion, Austin, TX). Total RNA concentrations were estimated by measuring the optical density. First-strand cDNA was synthesized from 1 μg of total RNA using reverse-transcriptase M-MLV (Takara, Shiga, Japan) and oligo-dT primers. The cDNA was then diluted with DEPC-treated water to a volume of 50 μl.

Quantitative real-time PCR was used to assay transcription factor and cytokine mRNA levels. β-actin was used as an endogenous control. The oligonucleotide primers used for the transcription factors, cytokines, and β-actin (5,10,16,33) are listed in Table 1. Amplification was done using an ABI/PRISM 7000 Sequence Detection System and Power SYBR Green PCR master mix (Applied Biosystems, Carlsbad, CA), with the following thermal profile: one cycle at 50 C for 2 min, one cycle at 95 C for 10 min, 45 cycles at 95 C for 15 sec, and one cycle at 60 C for 1 min. Each amplification reaction was performed in triplicate. The relative quantification of cytokine gene expression was done using the comparative threshold cycles (C_T) method. The C_T data for each cytokine were normalized using the β-actin data from the same sample.

Neutralizing antibody test. Neutralizing antibody titers were measured using the 80% plaque reduction neutralization test ($PRNT_{80}$). Sera were diluted serially in twofold steps from 1:20 to 1:640 in 96-well plates. Each serum dilution was then combined with an equal volume of WNV and adjusted to give a final count of ~50 PFU per well. The serum-virus mixtures were then incubated for 60 min at 37 C in a CO_2 incubator. After incubation, the mixtures were transferred to 12-well plates containing BHK-21 cell monolayers. The plates were incubated for 60 min at 37 C to allow virus adsorption. After removing the mixture, the cells were washed three times with PBS, 1 ml of CMC-EMEM was added, and the plates were incubated at 37 C in a CO_2 incubator for 3 days. CMC-EMEM was then aspirated. The cells were fixed and stained for 2 hr with 0.1% crystal violet and 10% formalin in PBS. Finally, the cells were washed and air-dried and the plaques were counted. The neutralizing antibody titers are expressed as the reciprocal of the highest dilution that reduced the number of plaques to 80% or less of the control value.

Statistical analysis. *P*-values were calculated using unpaired Student *t*-tests.

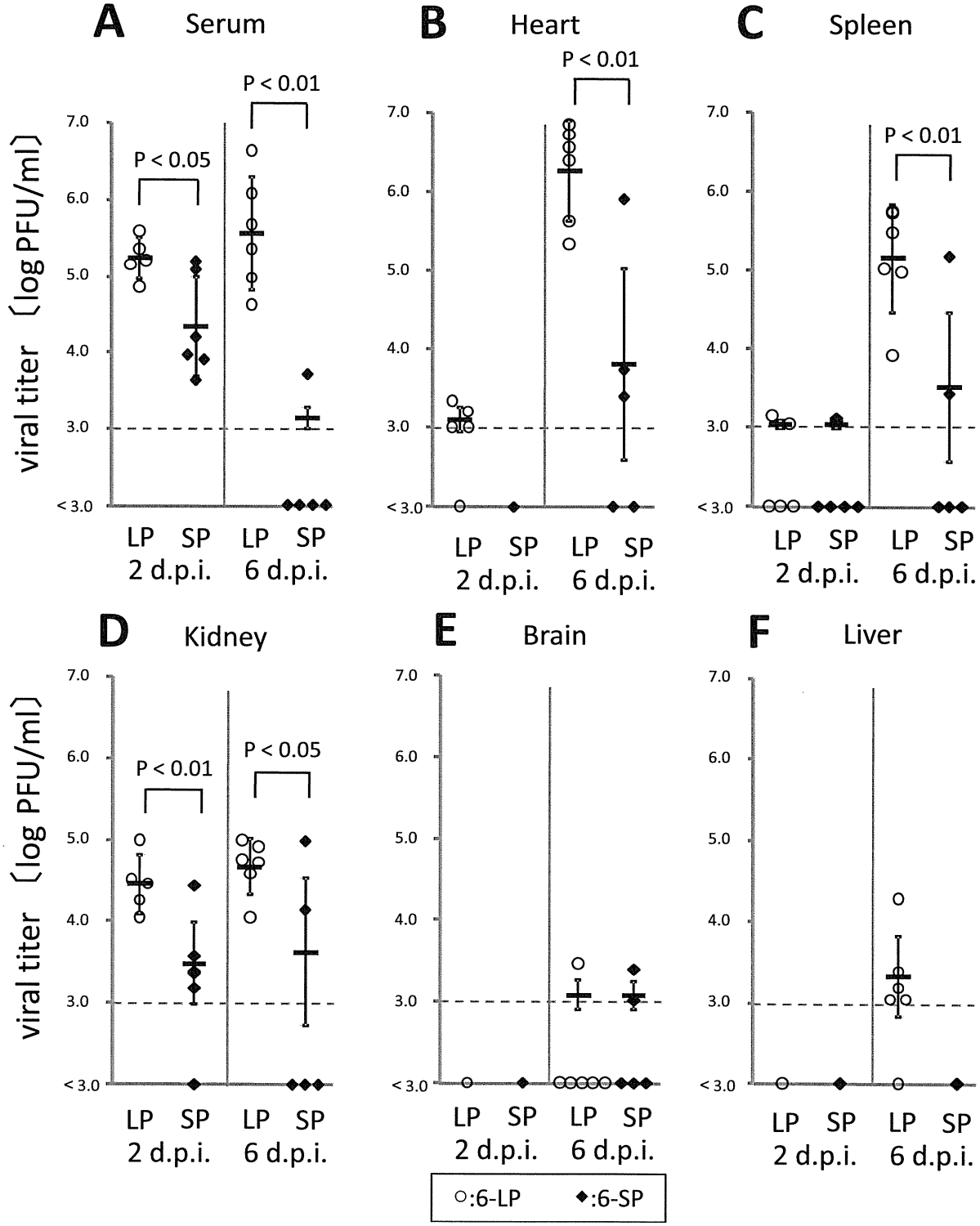

Fig. 1. Viral titers in the serum (A), hearts (B), spleens (C), kidneys (D), brains (E), and livers (F) of 2-day-old chicks infected with 6-LP (○) or 6-SP (◆). Chicks were infected with 10^2 PFU s.c. in the femoral region, and blood and tissues were collected at 2 and 6 d.p.i. Virus titers were determined by plaque assay using BHK-21 cells (n = 5 or 6). Individual and mean PFU values are represented by symbols and bars, respectively. When mean values were calculated, the titers of samples below the detection limit (10^3 PFU/ml) were considered to be 3.0. Error bars indicate standard deviations. P-values were calculated using unpaired Student t-tests.

RESULTS

Pathogenicity of WNV 6-LP and 6-SP in 2-day-old chicks. We previously demonstrated the presence of an N-linked glycosylation site in the E protein of WNV 6-LP, but not 6-SP, as a result of an amino acid substitution (27). Therefore, we used these two variants to analyze the effect of E protein glycosylation on WNV. Two-day-old chicks were inoculated subcutaneously with 100 PFU of WNV 6-LP or 6-SP. Blood and tissues were collected at 2 and 6 d.p.i. to observe the viral kinetics and host immune response.

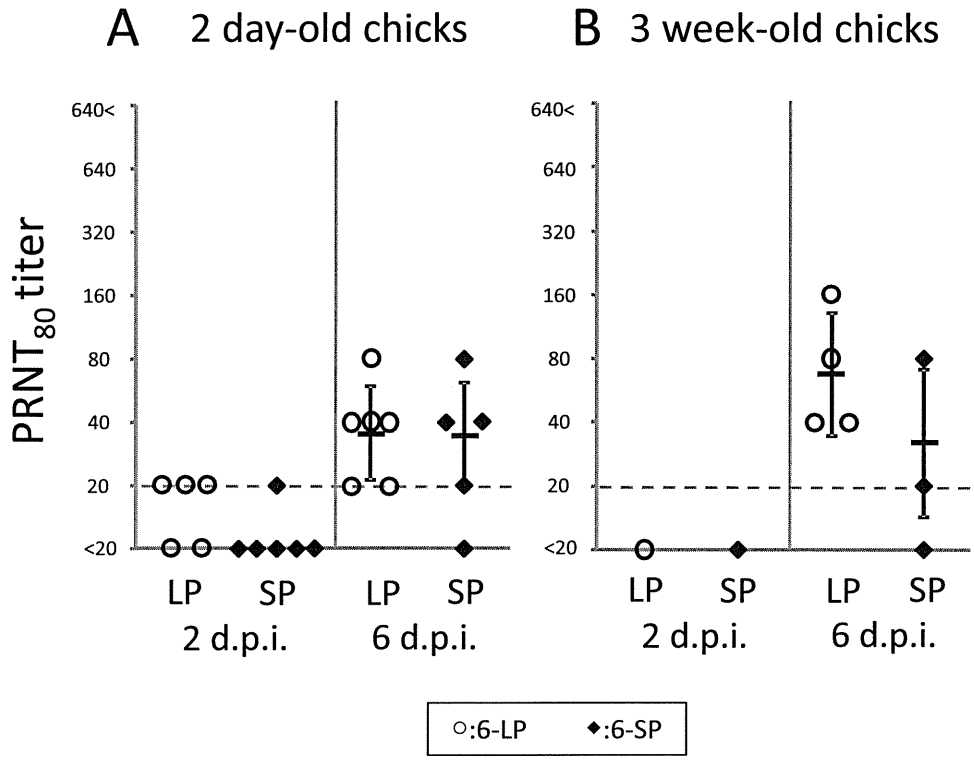

Fig. 2. Primary neutralizing antibody (Ab) responses in chicks inoculated with WNV 6-LP or 6-SP. Two-day-old (A) and 3-wk-old (B) chicks (n = 3–6) were inoculated with 10^2 PFU of WNV 6-LP (○) or 6-SP (◆). WNV neutralizing antibody titers were then measured by $PRNT_{80}$. Individual and mean $PRNT_{80}$ titers are represented by symbols and bars, respectively. When mean values were calculated, the titers of samples under the detection limit (20) were considered to be 20.

Eight of 18 chicks (44%) infected with 6-LP and two of 17 (12%) infected with 6-SP showed clinical signs of disease, including depression and weakening (data not shown). The 6-LP–infected chicks had significantly greater viremia than the 6-SP–infected chicks at 2 and 6 d.p.i. At 6 d.p.i., the viremia titers of the 6-LP–infected chicks exceeded 10^5 PFU/ml, while the 6-SP–infected chicks showed only a low level of viremia (Fig. 1A). The viral titers in the hearts, spleens, and kidneys of the 6-LP–infected chicks were significantly higher than those of the 6-SP–infected chicks at 6 d.p.i. (Fig. 1B–D). Low levels of virus were detected in the brains of both 6-LP– and 6-SP–infected chicks and in the liver of 6-LP–infected chicks (Fig. 1E,F).

Neutralizing antibody titers were measured using an 80% plaque reduction neutralizing test. Neutralizing antibodies were not detected in any chicks at 2 d.p.i., but they were detected at 6 d.p.i. in chicks infected with both 6-LP and 6-SP (Fig. 2A). However, the neutralizing antibody response in the 6-LP– and 6-SP–infected chicks was not significantly different.

To examine the involvement of cytokines and transcription factors in WNV pathogenicity, the expression of interferon-α (IFN-α), lipopolysaccharide-induced TNF-α factor (LITAF), tumor necrosis factor superfamily 15 (TNFSF15), interleukin (IL)–1β, IL-6, and IFN-γ was measured by real-time PCR. TNFSF15 has been reported to act as an inflammatory cytokine in chicks, similar to mammalian tumor necrosis factor (TNF)–α (20,33), and LITAF induced the expression of TNFSF15 in chicken macrophages (8). In the hearts and spleens of chicks inoculated with 6-LP and 6-SP, the transcription factor and the cytokine expression were higher than those observed in mock-infected chicks ($P < 0.01$; Fig. 3A,B). However, there was no significant difference in cytokine expression between the 6-LP– and 6-SP–infected chicks. No difference was observed in transcription factor or cytokine expression in clots from WNV-infected chicks and the mock-infected chicks (data not shown).

Pathogenicity of WNV 6-LP and 6-SP in 3-wk-old chicks. The susceptibility of adult chickens to WNV is low (15,21). To analyze the effect of glycosylation of the E protein on pathogenicity in older chicks, 3-wk-old chicks were inoculated with WNV 6-LP or 6-SP. No clinical symptoms were observed and no virus was detected in chicks infected with either variant (data not shown). Neutralizing antibody titers were detected in chicks infected with 6-LP and 6-SP at 6 d.p.i. (Fig. 2B). However, no significant difference in the neutralizing antibody response was detected between 6-LP and 6-SP or between 2-day-old and 3-wk-old chicks. Cytokine expression in the spleens of the WNV-infected chicks was significantly higher than that in mock-infected chicks (Fig. 4) and was similar to that in the 2-day-old chicks (Fig. 3B).

DISCUSSION

Birds play an important role in the transmission of WNV in nature; however, the pathogenicity of this virus in birds remains unclear. Thus, understanding the transmission and pathogenicity of WNV in birds is vital for the establishment of efficient preventive measures. In this study, young domestic chicks were infected with WNV, and the effect of E protein glycosylation on pathogenicity was determined. The glycosylated variant caused high viremia ($>10^5$ PFU/ml) in 2-day-old chicks, and high levels of virus were detected in the hearts, spleens, and kidneys. In contrast, lower viremia and low levels of virus in organs were observed in chicks infected with the nonglycosylated variant. These data indicated that the glycosylation of the E protein is important for multiplication in peripheral organs.

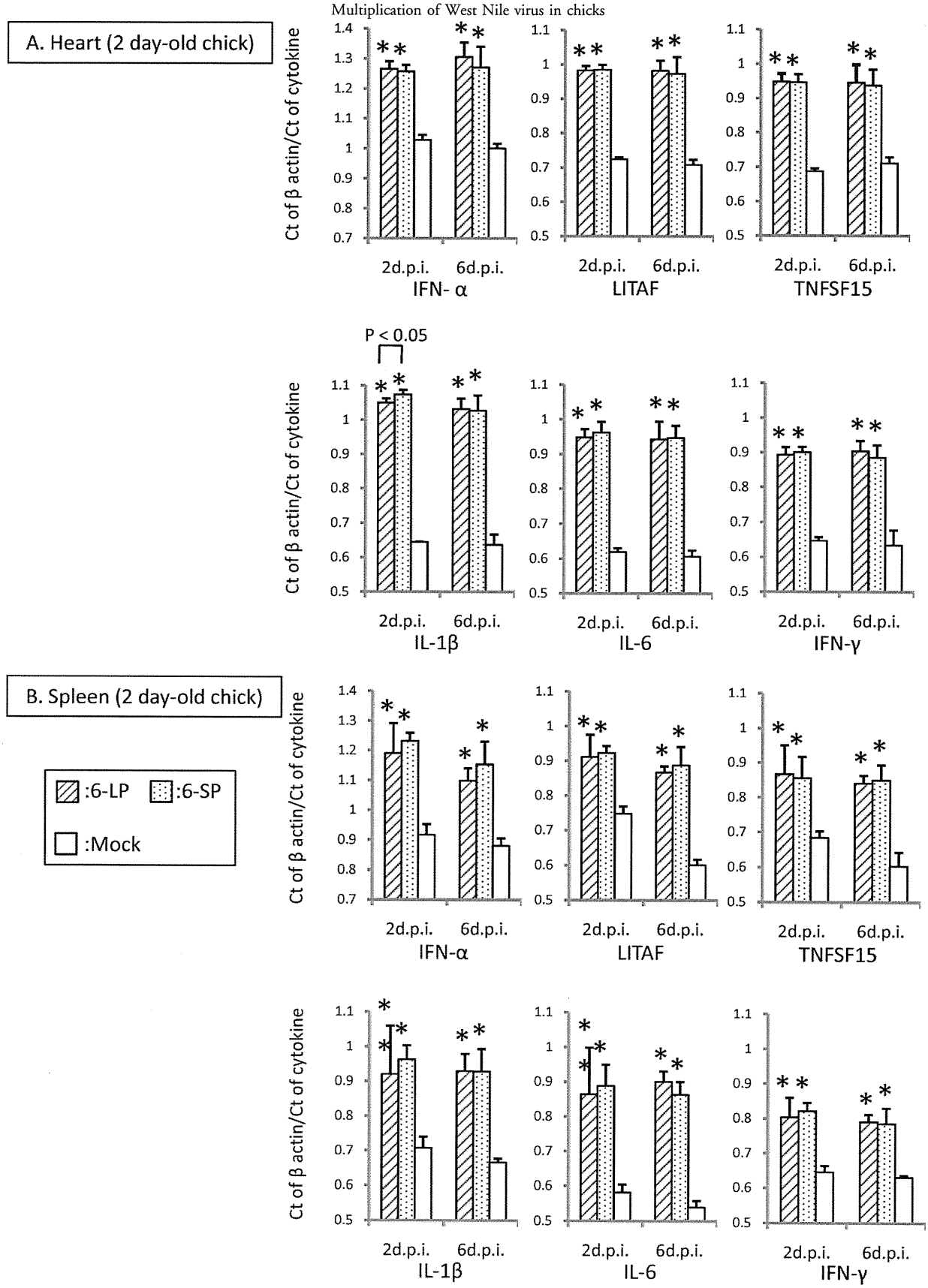

Fig. 3. Cytokine and transcription factor mRNA levels in the hearts (A) and spleens (B) of 2-day-old chicks inoculated with WNV 6-LP or 6-SP. Chicks were infected with 10^2 PFU of virus administered subcutaneously in the femoral region, and tissues were collected at 2 and 6 d.p.i. Total RNA was then extracted and cDNA synthesized. SYBR Green–based quantitative real-time PCR was performed using the synthesized cDNA. Relative quantification of cytokine gene expression was done using the C_T method. The C_T data for each cytokine were normalized against the β-actin levels in the same sample. * and ** indicate statistically significant differences (* $P < 0.01$; ** $P < 0.05$) in cytokine and transcription factor mRNA levels compared with mock-infected chicks.

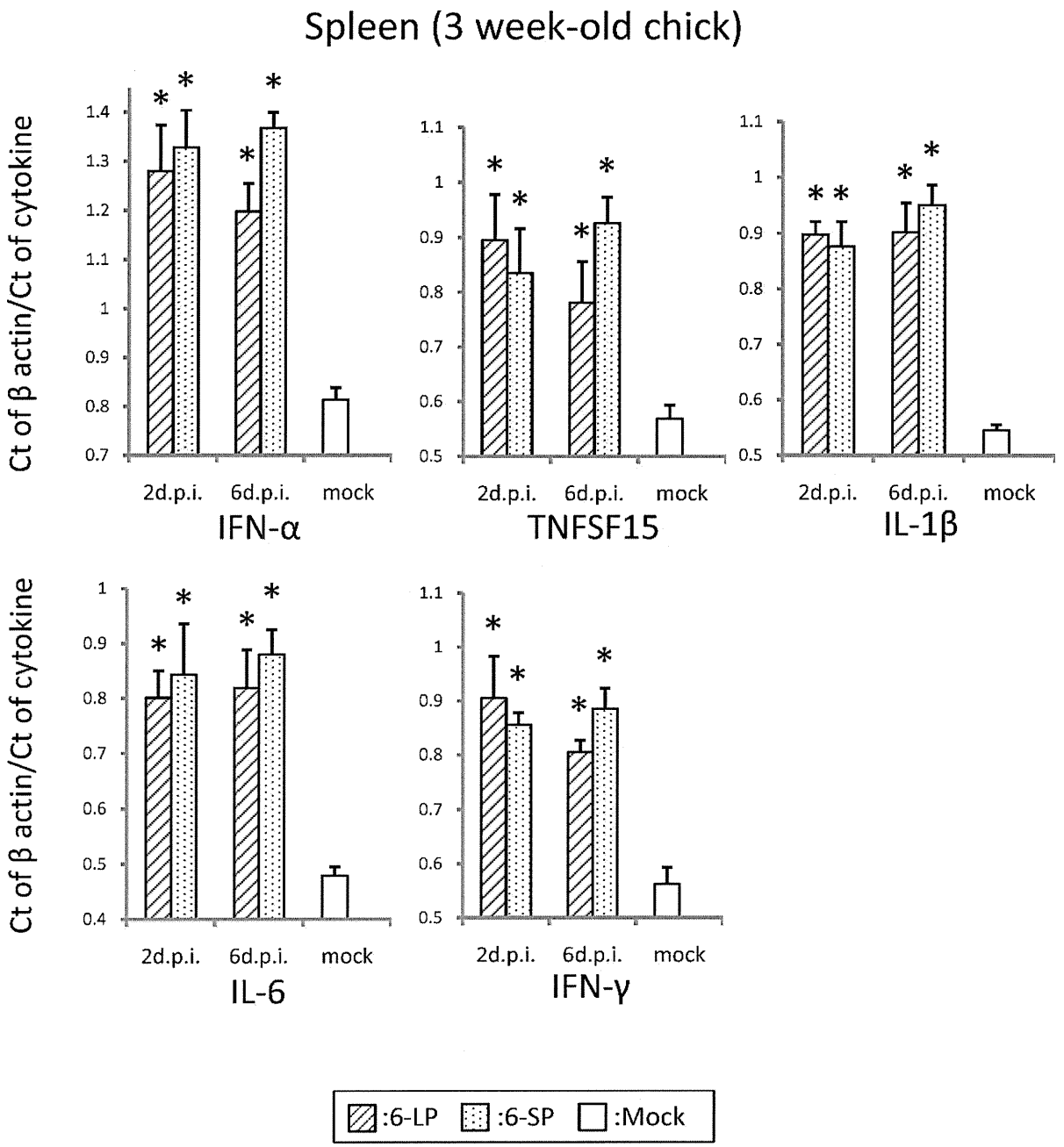

Fig. 4. Cytokine and transcription factor mRNA levels in the spleens of 3-wk-old chicks inoculated with WNV 6-LP or 6-SP. Chicks were infected with 10^2 PFU s.c. in the femoral region, and tissues were collected at 2 and 6 d.p.i. Total RNA was extracted and cDNA synthesized. SYBR Green–based quantitative real-time PCR was performed using the synthesized cDNA. Relative quantification of cytokine gene expression was done using the C_T method. The C_T data for each cytokine were normalized against the β-actin levels in the same sample. * Statistically significant differences ($P < 0.01$) in cytokine and transcription factor mRNA levels compared with mock-infected chicks.

High levels of viremia were also reported in American crows (3,12). Previous studies (34) have shown that avian viremic levels exceeding 10^5 PFU/ml are crucial for efficient infection of the insect vector, *Culex pipiens* mosquitoes. Therefore, these data indicate that young domestic chicks may contribute to the transmission of WNV in nature.

In this study, the highest virus titers were detected in the heart, and we previously showed (18) severe necrotic myocarditis in the hearts of 2-day-old chicks after infection with 6-LP. WNV multiplication and various degrees of cardiac lesions have been reported in dead wild birds (31,36). These data indicate that the heart is one of the major targets of WNV in birds. Virus was also detected in the spleens and kidneys of dead wild birds and in young chicks in this study. Thus, viral multiplication in peripheral organs, particularly the heart, contributes to the pathogenicity of WNV in birds.

No virus was detected in the brains, and no neurologic signs were observed in 2-day-old chicks infected with WNV. Encephalitis has been reported in WNV-infected mammals (22,28) and several species of birds (e.g., American crows [3] and young domestic geese [32]). These differences indicate that the neuroinvasiveness of WNV varies depending on the species.

Higher levels of virus were detected in the blood and peripheral organs of 2-day-old chicks infected with the glycosylated WNV

variant. Glycosylation of the E protein has been reported to enhance viral multiplication in mammalian and avian cells (2,17,18,27) and to be involved in the stability of the virion at mildly acidic pH (2). In a mouse model, glycosylated WNV caused stronger viremia and higher neuroinvasiveness than did nonglycosylated WNV, resulting in the enhanced virulence (2,27). In our previous study (18), glycosylation of the E proteins was shown to increase mortality in young domestic chicks. Therefore, glycosylation of the E protein of WNV enhanced viral multiplication in peripheral organs, leading to the strong pathogenicity of the virus in birds.

Host immune responses were not significantly different in 2-day-old and 3-wk-old chicks after infection with either 6-LP or 6-SP. In several mouse model studies, the involvement of various pro-inflammatory cytokines in pathogenicity has been reported, such as immune-mediated tissue damage caused by the expression of TNF-α (35) and the protection against WNV by TNF-α (30), IFN-γ (29), and IFN-α/β (23). However, our data indicate that the immune response may not affect the pathogenicity of, or protection against, WNV infection in birds. Since the cytokine response to viral infection in birds is not well understood, it is possible that other cytokines or chemokines are involved in the response to WNV infection.

No virus was detected in the blood and organs of 3-wk-old chicks, although neutralizing antibodies and cytokine responses were induced. These data indicate that the virus was cleared at an early stage of infection, prior to multiplication in organs. A similar low susceptibility to WNV was reported in older chicks and adult chickens (15,21,26). It is thus possible that susceptibility to WNV changed as the chicks grew, leading to lower viral multiplication.

In summary, we analyzed the effect of glycosylation of the E protein of WNV on pathogenicity in young domestic chicks. The glycosylated variant of WNV was more highly pathogenic, indicating the utility of the young chick model of WNV infection. Glycosylation of the E protein was shown to enhance viral multiplication in the blood and peripheral organs, which is itself associated with high pathogenicity. Our data will contribute to a greater understanding of WNV pathogenicity in birds and will facilitate more effective control measures and the prevention of WNV.

REFERENCES

1. Anderson, J. F., T. G. Andreadis, C. R. Vossbrinck, S. Tirrell, E. M. Wakem, R. A. French, A. E. Garmendia, and H. J. Van Kruiningen. Isolation of West Nile virus from mosquitoes, crows, and a Cooper's hawk in Connecticut. Science 286:2331–2333. 1999.

2. Beasley, D. W., M. C. Whiteman, S. Zhang, C. Y. Huang, B. S. Schneider, D. R. Smith, G. D. Gromowski, S. Higgs, R. M. Kinney, and A. D. Barrett. Envelope protein glycosylation status influences mouse neuroinvasion phenotype of genetic lineage 1 West Nile virus strains. J. Virol. 79:8339–8347. 2005.

3. Brault, A. C., S. A. Langevin, R. A. Bowen, N. A. Panella, B. J. Biggerstaff, B. R. Miller, and N. Komar. Differential virulence of West Nile strains for American crows. Emerg. Infect. Dis. 10:2161–2168. 2004.

4. Dauphin, G., S. Zientara, H. Zeller, and B. Murgue. West Nile: worldwide current situation in animals and humans. Comp. Immunol. Microbiol. Infect. Dis. 27:343–355. 2004.

5. De Boever, S., C. Vangestel, P. De Backer, S. Croubels, and S. U. Sys. Identification and validation of housekeeping genes as internal control for gene expression in an intravenous LPS inflammation model in chickens. Vet. Immunol. Immunopathol. 122:312–317. 2008.

6. Eidson, M., N. Komar, F. Sorhage, R. Nelson, T. Talbot, F. Mostashari, and R. McLean. Crow deaths as a sentinel surveillance system for West Nile virus in the northeastern United States, 1999. Emerg. Infect. Dis. 7:615–620. 2001.

7. Goto, A., K. Yoshii, M. Obara, T. Ueki, T. Mizutani, H. Kariwa, and I. Takashima. Role of the N-linked glycans of the prM and E envelope proteins in tick-borne encephalitis virus particle secretion. Vaccine 23:3043–3052. 2005.

8. Hong, Y. H., H. S. Lillehoj, S. H. Lee, D. W. Park, and E. P. Lillehoj. Molecular cloning and characterization of chicken lipopolysaccharide-induced TNF-alpha factor (LITAF). Dev. Comp. Immunol. 30:919–929. 2006.

9. Hubalek, Z., and J. Halouzka. West Nile fever—a reemerging mosquito-borne viral disease in Europe. Emerg. Infect. Dis. 5:643–650. 1999.

10. Kano, R., S. Konnai, M. Onuma, and K. Ohashi. Cytokine profiles in chickens infected with virulent and avirulent Marek's disease viruses: interferon-gamma is a key factor in the protection of Marek's disease by vaccination. Microbiol. Immunol. 53:224–232. 2009.

11. Komar, N. West Nile virus: epidemiology and ecology in North America. Adv. Virus Res. 61:185–234. 2003.

12. Komar, N., S. Langevin, S. Hinten, N. Nemeth, E. Edwards, D. Hettler, B. Davis, R. Bowen, and M. Bunning. Experimental infection of North American birds with the New York 1999 strain of West Nile virus. Emerg. Infect. Dis. 9:311–322. 2003.

13. Komar, N., N. A. Panella, J. E. Burns, S. W. Dusza, T. M. Mascarenhas, and T. O. Talbot. Serologic evidence for West Nile virus infection in birds in the New York City vicinity during an outbreak in 1999. Emerg. Infect. Dis. 7:621–625. 2001.

14. Lanciotti, R. S., J. T. Roehrig, V. Deubel, J. Smith, M. Parker, K. Steele, B. Crise, K. E. Volpe, M. B. Crabtree, J. H. Scherret, R. A. Hall, J. S. MacKenzie, C. B. Cropp, B. Panigrahy, E. Ostlund, B. Schmitt, M. Malkinson, C. Banet, J. Weissman, N. Komar, H. M. Savage, W. Stone, T. McNamara, and D. J. Gubler. Origin of the West Nile virus responsible for an outbreak of encephalitis in the northeastern United States. Science 286:2333–2337. 1999.

15. Langevin, S. A., M. Bunning, B. Davis, and N. Komar. Experimental infection of chickens as candidate sentinels for West Nile virus. Emerg. Infect. Dis. 7:726–729. 2001.

16. Li, Y. P., K. J. Handberg, H. R. Juul-Madsen, M. F. Zhang, and P. H. Jorgensen. Transcriptional profiles of chicken embryo cell cultures following infection with infectious bursal disease virus. Arch. Virol. 152:463–478. 2007.

17. Moudy, R. M., B. Zhang, P. Y. Shi, and L. D. Kramer. West Nile virus envelope protein glycosylation is required for efficient viral transmission by Culex vectors. Virology 387:222–228. 2009.

18. Murata, R., Y. Eshita, A. Maeda, J. Maeda, S. Akita, T. Tanaka, K. Yoshii, H. Kariwa, T. Umemura, and I. Takashima. Glycosylation of the West Nile virus envelope protein increases in vivo and in vitro viral multiplication in birds. Am. J. Trop. Med. Hyg. 82:696–704. 2010.

19. Panella, N. A., A. J. Kerst, R. S. Lanciotti, P. Bryant, B. Wolf, and N. Komar. Comparative West Nile virus detection in organs of naturally infected American crows (Corvus brachyrhynchos). Emerg. Infect. Dis. 7:754–755. 2001.

20. Park, S. S., H. S. Lillehoj, Y. H. Hong, and S. H. Lee. Functional characterization of tumor necrosis factor superfamily 15 (TNFSF15) induced by lipopolysaccharides and Eimeria infection. Dev. Comp. Immunol. 31:934–944. 2007.

21. Phipps, L. P., R. E. Gough, V. Ceeraz, W. J. Cox, and I. H. Brown. Detection of West Nile virus in the tissues of specific pathogen free chickens and serological response to laboratory infection: a comparative study. Avian Pathol. 36:301–305. 2007.

22. Sampson, B. A., C. Ambrosi, A. Charlot, K. Reiber, J. F. Veress, and V. Armbrustmacher. The pathology of human West Nile virus infection. Hum. Pathol. 31:527–531. 2000.

23. Samuel, M. A., and M. S. Diamond. Alpha/beta interferon protects against lethal West Nile virus infection by restricting cellular tropism and enhancing neuronal survival. J. Virol. 79:13350–13361. 2005.

24. Scherret, J. H., J. S. MacKenzie, A. A. Khromykh, and R. A. Hall. Biological significance of glycosylation of the envelope protein of Kunjin virus. Ann. N. Y. Acad. Sci. 951:361–363. 2001.